HHS Public Access

Author manuscript

*Nat Cardiovasc Res*. Author manuscript; available in PMC 2022 August 31.

Published in final edited form as:

*Nat Cardiovasc Res*. 2022 February ; 1(2): 142–156. doi:10.1038/s44161-021-00016-2.

# Sigma non-opioid receptor 1 is a potential therapeutic target for long QT syndrome

**LouJin Song**[1,2,#], **Ramsey Bekdash**[1,2,#], **Kumi Morikawa**[1,#], **Jose R. Quejada**[1,2,#], **Alison D. Klein**[1], **Danielle Aina-Badejo**[1], **Kazushige Yoshida**[1], **Hannah E. Yamamoto**[1,3], **Amy Chalan**[1], **Risako Yang**[1,4], **Achchhe Patel**[1,5], **Dario Sirabella**[1,5], **Teresa M. Lee**[1,6], **Leroy C. Joseph**[7], **Fuun Kawano**[1], **Junco S. Warren**[8,9,10], **Rajesh K. Soni**[11], **John P. Morrow**[7], **Masayuki Yazawa**[1,2,*]

[1]Columbia Stem Cell Initiative, Department of Rehabilitation and Regenerative Medicine, Columbia University, New York, U.S.A.

[2]Department of Pharmacology, Columbia University, New York, U.S.A.

[3]Barnard College, New York, U.S.A.

[4]Colgate University, Hamilton, U.S.A.

[5]Department of Genetics and Development, Columbia University, New York, U.S.A.

[6]Department of Pediatrics, Columbia University, New York, U.S.A.

[7]Department of Medicine, Columbia University, New York, U.S.A.

[8]Nora Eccles Harrison Cardiovascular Research and Training Institute, University of Utah, Salt Lake City, U.S.A.

[9]Department of Internal Medicine, University of Utah School of Medicine, Salt Lake City, USA

[10]Division of Developmental Genetics, Institute of Resource Developmental and Analysis, Kumamoto University, Kumamoto, Japan



[*]To whom correspondence should be addressed: Masayuki Yazawa, Ph.D., Assistant Professor, Columbia Stem Cell Initiative, Department of Rehabilitation and Regenerative Medicine, Department of Pharmacology, Columbia University Irving Medical Center, 650 West 168th Street, William Black Building BB1109D/BB1108, New York, NY 10032, USA, Tel: +1 212 305 1890/1052, Fax: +1 212 342 3889, my2387@columbia.edu.

[#]The authors wish it to be known that, in their opinion, the first four authors should be regarded as joint First Authors

Author Contributions

L.S. and M.Y. conceived of and designed this project. L.S., R.B., K.M., J.R.Q. and M.Y. designed experiments. L.S., R.B., K.M., J.R.Q., A.D.K., D.A., K.Y., H.E.Y., A.C., R.Y., A.P., D.S., L.C.J., T.M.L., F.K. R.K.S., J.P.M. and M.Y. perform experiments and analyzed the data: M.Y. conducted whole cell patch clamp; R.K.S conducted proteomics; F.K conducted computational modeling. L.S., R.B., K.M., J.R.Q., J.W. and M.Y. interpreted the data. M.Y. wrote the manuscript. L.S., R.B., K.M., J.R.Q., D.A., T.M.L. and J.P.M. proofread and edited the manuscript. All authors approved the manuscript.

Competing interest statement

L.S., R.B., K.M., J.R.Q. and M.Y. (inventors) filed a patent (Attorney Docket No.: 01001/005273-US1; status: Filed, 10/04/2019) related to this manuscript. This patent is for using agonists of Sigma non-opioid receptor 1 for treating long QT syndrome (type 1, 2 and 8) and related cardiac channelopathy. The rest of the authors declare no competing interests.

Supplementary Movie 1 and 2

Representative time lapse phase contrast images of Timothy syndrome iPSC-derived cardiomyocyte clusters before (Move 1) and after 2-hr 5μM PRE-084 treatment (Movie 2). The analyses are shown in Ext. Fig. 1h–j. Red (left/bottom), a marker used for this cluster area.

[11]Proteomics and Macromolecular Crystallography Shared Resource, Columbia University, New York, U.S.A.

## Abstract

Some missense gain-of-function mutations in *CACNA1C* gene, encoding calcium channel $Ca_V1.2$, cause a life-threatening form of long QT syndrome named Timothy syndrome, with currently no clinically-effective therapeutics. Here we report that pharmacological targeting of sigma non-opioid intracellular receptor 1 (SIGMAR1) can restore electrophysiological function in iPSC-derived cardiomyocytes generated from patients with Timothy syndrome and two common forms of long QT syndrome, type 1 (LQTS1) and 2 (LQTS2), caused by missense trafficking mutations in potassium channels. Electrophysiological recordings demonstrate that an FDA-approved cough suppressant, dextromethorphan, can be used as an agonist of SIGMAR1, to shorten the prolonged action potential in Timothy syndrome cardiomyocytes and human cellular models of LQTS1 and LQTS2. When tested *in vivo*, dextromethorphan also normalized the prolonged QT intervals in Timothy syndrome model mice. Overall, our study demonstrates that SIGMAR1 is a potential therapeutic target for Timothy syndrome and possibly other inherited arrhythmias such as LQTS1 and LQTS2.

## Introduction

Calcium ions ($Ca^{2+}$) play an essential role in cardiac excitation-contraction coupling[1,2]. $Ca^{2+}$ handling dysfunction is associated with various cardiac arrhythmias and genetic syndrome such as long QT syndrome (LQTS)[3,4]. Some *de novo* gain-of-function mutations such as G406R in cardiac L-type voltage-gated calcium channel $Ca_V1.2$, which is encoded by *CACNA1C*, cause a lethal form of LQTS (type 8, also named Timothy syndrome, TS)[3,5]. Previously, using human patient-specific induced pluripotent stem cells (iPSCs), we found that the increased activity of cyclin-dependent kinase 5 (CDK5) is involved in the cardiac pathophysiological basis of TS (Figure 1a, red)[6]. In addition, we observed that inhibiting CDK5 using genetic approaches and chemical inhibitors, such as PHA-793887, alleviated the cellular phenotypes in the TS iPSC-derived cardiomyocytes[6]. However, currently-available inhibitors for CDK5 also show inhibitory effects on other cyclin-dependent kinases. As a result, if the inhibitors are used for clinical application for treating cardiac diseases, it may lead to adverse events[7] because cyclin-dependent kinases are known to play a critical role in cell-cycle regulation. Moreover, developing CDK5-specific inhibitor is challenging due to the structural similarity of the catalytic domain between different cyclin-dependent kinases[8]. Therefore, using small molecules to directly target CDK5 is not ideal for further translational development to fulfill the unmet medical needs of TS patients. For this reason, we decided to look for alternative approaches that may modulate CDK5 activity in human cardiomyocytes. A comprehensive literature search returned sigma non-opioid intracellular receptor 1 (SIGMAR1) as a potential target. SIGMAR1 is an emerging target for neurodegenerative diseases and cancer[9–11], playing an important role as a chaperone protein in endoplasmic reticulum membranes for regulating protein homeostasis, mitochondrial function, ion channel function and $Ca^{2+}$ handling[12]. More importantly, the activation of SIGMAR1 has been reported to suppress CDK5 activity in

rodent neurons[13], making SIGMAR1 activation an attractive alternative approach for CDK5 inhibition in TS models. Furthermore, the structure of SIGMAR1 has been uncovered[14], which greatly facilitated the identification of SIGMAR1 ligands and the understanding of the interactions between SIGMAR1 and its ligands. Several SIGMAR1 agonists have been identified, including a potent and specific agonist PRE-084[15] as well as several FDA-approved drugs such as fluvoxamine[16] and dextromethorphan[17–20] (Figure 1a,b and Ext. Figure 1a). However, to our knowledge, little is known regarding the role of SIGMAR1 in cardiac ion channel regulation and pathophysiological conditions in cardiac arrhythmias. In this study, we examined the role of SIGMAR1 in the pathogenesis of LQTS as a therapeutic target and tested the hypothesis that the treatment of a SIGMAR1 agonist, such as PRE-084, fluvoxamine or dextromethorphan, could rescue cardiac phenotypes in TS (Figure 1a, blue).

## Results

### Effects of SIGMAR1 activation on TS cardiomyocytes

To examine whether SIGMAR1 activation modulates CDK5 activity in human cardiomyocytes as it did in neurons[13], we conducted an *in vitro* luminescence-based CDK5 activity assay[6] using TS patient-specific iPSC-derived cardiomyocytes treated with the SIGMAR1-selective agonist PRE-084. The results indicated that 2-hr PRE-084 treatment significantly reduced CDK5 activity in TS cardiomyocytes (Ext. Figure 1b). While it was reported that the protein expression of a CDK5-specific activator, CDK5R1/p35, was regulated by SIGMAR1 in neurons[13], interestingly, we observed no significant change in p35 protein expression between TS cardiomyocytes with and without PRE-084 treatment (Ext. Figure 1c,d). Instead, the protein expression of CDK5 was significantly reduced in TS cardiomyocytes treated with PRE-084 while no significant changes of CDK5 transcripts were detected (Ext. Figure 1c–e). These results revealed that the activation of SIGMAR1 using its selective agonist PRE-084 could modulate CDK5 activity in TS cardiomyocytes. To further explore the molecular mechanism underlying PRE-084-induced CDK5 reduction, we conducted a proximity ligation assay (PLA) to investigate the potential interaction between SIGMAR1 and CDK5. We found that SIGMAR1 directly interacted with CDK5 in TS cardiomyocytes and the treatment of PRE-084 significantly increased the number of SIGMAR1-CDK5 PLA signals in TS cardiomyocytes, indicating an increased interaction between SIGMAR1 and CDK5 under SIGMAR1 activation (Ext. Figure 1f,g). To validate that the change induced by PRE-084 was mediated by SIGMAR1, we treated TS cardiomyocytes with a potent and selective SIGMAR1 antagonist NE-100[21–23] along with PRE-084 and used the cells for SIGMAR1-CDK5 PLA. The results showed that the co-treatment of NE-100 with PRE-084 reversed the effect of PRE-084 on the interaction of SIGMAR1 and CDK5 in TS cardiomyocytes, confirming that the effect of PRE-084 was indeed mediated by SIGMAR1 (Ext. Figure 1f,g). Overall, the results indicated that SIGMAR1 directly interacted with CDK5 in TS cardiomyocytes and SIGMAR1 activation led to an increased interaction between SIGMAR1 and CDK5, and a reduced CDK5 expression and activity in TS cardiomyocytes.

The positive effect of SIGMAR1 activation on CDK5 activity prompted us to examine the effects of the SIGMAR1 agonist PRE-084 on the cellular phenotypes in TS cardiomyocytes.

We first examined the effect of PRE-084 on the irregular and slow contraction phenotype in TS cardiomyocytes using a contraction assay reported previously[6]. This is because, as the heart beating is normally regular, irregular contractions of cellular model indicate electrophysiological instability. The imaging results demonstrated that PRE-084 alleviated the irregular contraction and increased the beating rate of the patient cardiomyocytes (Ext. Figure 1h–j and Supplementary Movie 1 and 2). Next, we conducted whole-cell voltage clamp recordings to evaluate the effect of PRE-084 on the phenotype in voltage-dependent inactivation of $Ca_V1.2$ channel in TS cardiomyocytes. The result showed that PRE-084 treatment rescued the affected voltage-dependent inactivation of $Ca_V1.2$ in TS cardiomyocytes with 2-hr treatment but not acute (<10min) treatment (Ext. Figure 1k–n), supporting the beneficial effect of PRE-084 on TS cardiomyocytes. Furthermore, we examined the effect of PRE-084 on the prolonged action potential in TS cardiomyocytes and observed that PRE-084 significantly shortened the prolonged action potentials in the patient cardiomyocytes (Figure 1c,d and Ext. Figure 2a–c). Overall, these results demonstrated that the selective SIGMAR1 agonist PRE-084 ameliorated the phenotypes in TS cardiomyocytes. This points to SIGMAR1 activation as a potential therapeutic avenue for the cardiac phenotypes in TS.

Next, we examined the effects of fluvoxamine and dextromethorphan, which are also SIGMAR1 agonists, on the phenotypes in TS cardiomyocytes. FDA-approved drugs, fluvoxamine and dextromethorphan, may have a greater translational potential for TS if the drugs are proved to be effective on the human cellular model. Similar to the selective SIGMAR1 agonist PRE-084, electrophysiological recordings revealed that the SIGMAR1 agonists, fluvoxamine and dextromethorphan, restored $Ca_V1.2$ voltage-dependent inactivation and action potentials in TS cardiomyocytes (Figure 1c,d, Ext. Figure 1k,l, and Ext. Figure 2a–c).

At the dose that fluvoxamine and dextromethorphan rescued the electrophysiological phenotypes in TS cardiomyocytes, the two FDA-approved drugs did not significantly alter the action potential duration of normal cardiomyocytes generated from isogenic control iPSC lines in which the TS mutation was previously corrected by gene editing technology[6] (Figure 1e,f and Ext. Figure 2d–f). We sought to understand the difference in the sensitivity to the treatment of SIGMAR1 agonists between normal and TS cardiomyocytes. It was found that at baseline there was a significant increase in SIGMAR1 transcripts and proteins in TS cardiomyocytes compared with normal cardiomyocytes (Ext. Figure 2g–j), which may predispose TS cardiomyocytes to respond to SIGMAR1 agonists. To further explore the upstream pathway that regulates the expression of SIGMAR1, we examined the expression of ATF4, a transcription factor that has been reported to directly regulate SIGMAR1 transcription[24]. The results demonstrated that there was a significant increase in ATF4 proteins (both non-phosphorylated and phosphorylated forms) and a significant decrease in ubiquitinated ATF4 protein in TS cardiomyocytes compared with their isogenic control cardiomyocytes (Ext. Figure 2k–n), indicating an accumulation of ATF4 protein in TS cardiomyocytes. To confirm the regulatory role of ATF4 on SIGMAR1 expression in human cardiomyocytes, we overexpressed ATF4 in human normal cardiomyocytes and conducted quantitative RT-PCR (qPCR) and Western blotting to examine the effect of increased ATF4 expression on SIGMAR1 mRNA and protein expressions. The results showed that ATF4

overexpression significantly increased the expression of SIGMAR1 transcript and protein in human iPSC-derived cardiomyocytes (Ext. Figure 2o–r), confirming the regulation of SIGMAR1 expression via ATF4. Altogether, the results suggest that the increased ATF4 proteins in TS cardiomyocytes might activate the transcription of SIGMAR1 and upregulate the expression of SIGMAR1, leading to an increased sensitivity of TS cardiomyocytes to the treatment of SIGMAR1 agonists.

Although the observed beneficial effects of fluvoxamine and dextromethorphan on TS cardiomyocytes were both encouraging, dextromethorphan seems to hold greater therapeutic potential for translational application because of its wider age range for clinical usage and favorable safety profile when used appropriately[16,20,25–27]. Thus, we decided to further characterize the effects of dextromethorphan. To examine the effect of dextromethorphan on the abnormal $Ca^{2+}$ handling phenotype in TS cardiomyocytes, we used a genetically encoded fluorescent $Ca^{2+}$ indicator, GCaMP6f[28], for $Ca^{2+}$ imaging. Compared with using $Ca^{2+}$ dyes such as Fluo-4 AM, $Ca^{2+}$ imaging using genetically encoded indicators has the distinct advantage that infected cells are intact and remain in reliable imaging condition for hours, which enables continuous monitoring of changes in $Ca^{2+}$ handling after compound treatment for a longer time. Consistent with our previous findings using Fluo-4 AM for $Ca^{2+}$ imaging[5], $Ca^{2+}$ imaging using GCaMP6f confirmed that TS cardiomyocytes demonstrated abnormal $Ca^{2+}$ handling compared with the isogenic control cardiomyocytes, and this phenotype can be stably monitored for at least two hours after GCaMP6f fluorescent imaging started (Ext. Figure 3a–d). Using GCaMP6f-based $Ca^{2+}$ imaging, we found that dextromethorphan treatment exhibited significant beneficial effects on the abnormal $Ca^{2+}$ handling phenotype in TS cardiomyocytes and significantly increased $Ca^{2+}$ transient frequency and shortened $Ca^{2+}$ transient duration at 2 hours after treatment (Figure 2a–c), which is also the time point that we observed a significant beneficial effect of dextromethorphan on the electrophysiological phenotypes in TS cardiomyocytes (Figure 1c,d).

Next, to further characterize the effect of dextromethorphan on the L-type calcium channel function in TS cardiomyocytes, we conducted whole-cell voltage clamp recordings using $Ca^{2+}$ as the charge carrier to examine the effect of dextromethorphan on the calcium channel currents. We found that dextromethorphan significantly reduced late calcium currents in TS cardiomyocytes (Figure 2d,e). This result along with the result from the electrophysiological recordings using $Ba^{2+}$ as the charge carrier (Ex. Figure 1l and Ext. Figure 3e) demonstrated that dextromethorphan restored the inactivation of $Ca_V1.2$ channel in TS cardiomyocytes. In addition, to validate that the effect of dextromethorphan on $Ca_V1.2$ channel inactivation was mediated by SIGMAR1, we tested the selective SIGMAR1 antagonist NE-100[21–23] along with dextromethorphan in the electrophysiological recordings using $Ba^{2+}$ as the charge carrier. We found that the beneficial effect of dextromethorphan on the affected voltage-dependent inactivation of $Ca_V1.2$ in TS cardiomyocytes was reversed by the co-treatment of NE-100, indicating that the beneficial effect of dextromethorphan on calcium channel inactivation was mediated by SIGMAR1 (Figure 2f,g). On the other hand, at its efficacious dose on TS cardiomyocytes, dextromethorphan did not significantly alter the voltage-dependent inactivation of $Ca_V1.2$ in their isogenic control cardiomyocytes (Ext. Figure 3f,g). Furthermore, since SIGMAR1 has been reported to interact with L-type

calcium channels and regulate channel function in retinal ganglion cells and dorsal ganglion neurons[29–31], we examined the potential interaction between SIGMAR1 and $Ca_V1.2$ in TS cardiomyocytes and the effect of dextromethorphan on the interaction using PLA. The results suggest that SIGMAR1 directly interacted with $Ca_V1.2$ in TS cardiomyocytes and there was a significant reduction in the number of SIGMAR1-$Ca_V1.2$ PLA signals in TS cardiomyocytes after dextromethorphan treatment (Ext. Figure 3h,i), indicating that dextromethorphan reduced the direct interaction between SIGMAR1 and $Ca_V1.2$ in TS cardiomyocytes. Altogether, the results demonstrated that dextromethorphan restored the channel inactivation of $Ca_V1.2$ in TS cardiomyocytes through SIGMAR1 activation. The findings in aggregate indicated that SIGMAR1 might play a multifaceted role in regulating $Ca_V1.2$ channel function in human iPSC-derived cardiomyocytes by not only regulating CDK5 activity but also directly interacting with $Ca_V1.2$.

To further investigate the effect of dextromethorphan on cardiac action potential, we performed voltage-clamp recordings to measure hERG currents in TS cardiomyocytes because potassium ion ($K^+$) channels are also known to play an important role in the repolarization phase of action potential in cardiomyocytes. Interestingly, we found that there was a significant reduction of $I_{Kr}$ currents in TS cardiomyocytes compared with isogenic control cardiomyocytes (Ext. Figure 3j–l). Moreover, dextromethorphan treatment significantly increased $I_{Kr}$ steady-state amplitude in TS cardiomyocytes while no significant change of $I_{Kr}$ currents was observed for the isogenic control cardiomyocytes treated with dextromethorphan at the same dose (Figure 2h,i, Ext. Figure 3l and Ext. Figure 4a–c). Furthermore, the beneficial effect of dextromethorphan on $I_{Kr}$ currents in TS cardiomyocytes was blocked by the co-treatment of SIGMAR1 antagonist NE-100 with dextromethorphan, confirming that the effect of dextromethorphan on hERG channels was mediated by SIGMAR1 (Figure 2h,i and Ext. Figure 3l,m). These results suggest that SIGMAR1 activation mediated by dextromethorphan might rescue the prolonged action potentials in TS cardiomyocytes by restoring $K^+$ efflux in addition to reducing $Ca^{2+}$ influx.

SIGMAR1 has been reported to directly interact with hERG channel in HEK cells[32] and the direct interaction was further confirmed by atomic force microscopy[33]. In addition, SIGMAR1 silencing using shRNA or the treatment of progesterone, which is also known as a SIGMAR1 antagonist, decreased hERG current density and negatively regulated the membrane expression of hERG channel in leukemic cells, HEK cells and neonatal rat cardiomyocytes[12,32,34] while SIGMAR1 overexpression potentiated hERG current density in Xenopus oocytes[32]. Thus, we decided to evaluate the potential interaction between SIGMAR1 and hERG channel in human iPSC-derived cardiomyocytes using PLA and examine the effect of dextromethorphan on their potential interaction. We found that consistent with the previous report using HEK cells[32], SIGMAR1 also directly interacted with hERG channel in human iPSC-derived cardiomyocytes. Two-hour dextromethorphan treatment significantly reduced SIGMAR1-hERG PLA signals in TS cardiomyocytes while no significant change of SIGMAR1-hERG PLA signals in the isogenic control cardiomyocytes was observed with dextromethorphan treatment at the same dose (Figure 2j,k and Ext. Figure 4d–g).

To investigate the molecular mechanisms underlying the effect of dextromethorphan on hERG channel further, we conducted immunocytochemistry for hERG channel and plasma membrane with the hERG antibody and the Wheat Germ Agglutinin (WGA) fluorescent dye, respectively, using TS cardiomyocytes with and without the treatment of dextromethorphan. We imaged the stained cardiomyocytes using a confocal microscope and then conducted blinded quantification for the co-localization of hERG and WGA fluorescent signals, in order to examine the effect of dextromethorphan on the membrane localization of hERG in TS cardiomyocytes. The result suggest that there was a trend towards an increased hERG-WGA co-localization in dextromethorphan-treated TS cardiomyocytes compared with non-treated ones while the change did not reach statistical significance (Ext. Figure 5a,b). In addition, we explored the possibility that SIGMAR1 activation induced by dextromethorphan increased the expression of *KCNH2*/hERG, resulting in the increased $I_{Kr}$ observed in TS cardiomyocytes. Therefore, qPCR and Western blotting were conducted to examine the expression of *KCNH2*/hERG transcript and protein in TS cardiomyocytes with or without dextromethorphan treatment. We found that dextromethorphan significantly increased hERG/*KCNH2* transcription in the patient cardiomyocytes (Ext. Figure 5c) and did not significantly alter the protein expression of hERG (Ext. Figure 5d,e).

Overall, these results demonstrated that SIGMAR1 directly interacted with hERG channel in human iPSC-derived cardiomyocytes and the SIGMAR1 agonist dextromethorphan might increase $I_{Kr}$ currents by dissociating the interaction between SIGMAR1 and hERG channel in TS cardiomyocytes, while the exact mechanisms remain to be characterized.

The observation of an interaction between SIGMAR1 and hERG channel in human iPSC-derived cardiomyocytes prompted us to examine whether there is a similar interaction between SIGMAR1 and another $K^+$ channel, $K_V7.1$, which is encoded by *KCNQ1* gene and also plays an important role in the repolarization phase of cardiac action potential as hERG channel does. Utilizing electrophysiological recordings, we found that similar to our observations on hERG channel, TS cardiomyocytes showed significantly-reduced $I_{Ks}$ currents compared with the isogenic controls and the treatment of dextromethorphan significantly increased $I_{Ks}$ currents in TS cardiomyocytes (Figure 2l,m and Ext. Figure 5f,g). In addition, co-treatment of NE-100 with dextromethorphan blocked the beneficial effect of dextromethorphan on $I_{Ks}$ currents in TS cardiomyocytes, confirming that the effect of dextromethorphan on $K_V7.1$ channel is mediated by SIGMAR1 (Figure 2l,m and Ext. Figure 5g). Moreover, consistent with our observations for SIGMAR1 and hERG channel, SIGMAR1 also directly interacted with $K_V7.1$ channel in human iPSC-derived cardiomyocytes. Similarly, dextromethorphan treatment significantly reduced SIGMAR1-$K_V7.1$ PLA signals in TS cardiomyocytes (Figure 2n,o). On the other hand, there were no significant changes of $I_{Ks}$ currents in the isogenic control cardiomyocytes after dextromethorphan treatment at the same dose although a reduction in SIGMAR1-$K_V7.1$ PLA signals was observed upon the treatment (Ext. Figure 4h–k).

To investigate the molecular mechanisms underlying the effect of dextromethorphan on $K_V7.1$ channel further, we conducted immunocytochemistry for *KCNQ1*/$K_V7.1$ channel and plasma membrane using an $K_V7.1$ antibody and the WGA fluorescent dye, respectively, using TS cardiomyocytes with and without dextromethorphan treatment. A

significant increase in plasma-membrane localization of $K_V7.1$ channel was observed upon dextromethorphan treatment (Ext. Figure 5h,i), indicating that SIGMAR1 activation induced by dextromethorphan facilitated the membrane localization of $K_V7.1$ channels in TS cardiomyocytes. In addition, we conducted qPCR to examine the expression of *KCNQ1* transcripts in TS cardiomyocytes with and without dextromethorphan treatment, and observed a significant increase in the transcription of *KCNQ1* isoform 1 upon dextromethorphan treatment while the transcription of *KCNQ1* isoform 2 was not significantly altered by dextromethorphan treatment (Ext. Figure 5j). Consistent with the qPCR result, Western blotting showed a significant increase in the expression of $K_V7.1$ isoform 1 protein but not isoform 2 protein upon dextromethorphan treatment (Ext. Figure 5k–m), indicating that SIGMAR1 activation induced by dextromethorphan increased the expression of $K_V7.1$ isoform 1 in addition to facilitating the membrane localization of $K_V7.1$ channels.

In summary, these results demonstrated that, in addition to hERG channel, SIGMAR1 also directly interacted with $K_V7.1$ channel in human iPSC-derived cardiomyocytes and the SIGMAR1 agonist dextromethorphan might increase $I_{Ks}$ currents in TS cardiomyocytes by dissociating the interaction between SIGMAR1 and $K_V7.1$ channel, increasing the plasma-membrane localization of $K_V7.1$ and increasing the expression of $K_V7.1$ isoform 1.

## Effects of SIGMAR1 activation on LQTS1&2 cardiomyocytes

The observation that dextromethorphan increased $I_{Kr}$ and $I_{Ks}$ currents in TS cardiomyocytes motivated us to examine the effect of dextromethorphan on human iPSC-derived cardiomyocytes of two common types of LQTS, LQTS type 1 (LQTS1) and LQTS type 2 (LQTS2), carrying missense trafficking mutations G269S in $K_V7.1$ channel and A561V in hERG channel, respectively. The missense trafficking mutations in $K_V7.1$ and hERG channel have been reported previously to decrease $K^+$ currents and prolong action potentials in human iPSC-derived cardiomyocytes[35,36]. We first used CRISPR/Cas9 gene-editing technology to correct the mutations in our LQTS1 and LQTS2 iPSCs and generated isogenic control iPSCs (Ext. Figure 6a–d). Next, we differentiated both LQTS1 and LQTS2 iPSCs along with their corresponding isogenic controls to cardiomyocytes and evaluated their electrophysiological phenotypes. Consistent with previous reports[35,36], we found that both LQTS1 and LQTS2 iPSC-derived cardiomyocytes showed prolonged action potentials (APD90, 90% from peak, mean±s.d.: LQTS1 vs the isogenic control, 904.3±337.0ms vs 522.9±186.6ms, $p$=0.004; LQTS2 vs the isogenic control, 1,054.2±398.9ms vs 644.8±201.9ms, $p$=0.011, unpaired two-tailed Student's $t$-test) and also that the LQTS1/2 cardiomyocytes showed significantly-reduced $K^+$ currents in electrophysiological recordings compared with their corresponding isogenic control cardiomyocytes (Ext. Figure 6j,k,q–s). The treatment of a SIGMAR1 agonist, fluvoxamine or dextromethorphan, significantly shortened the prolonged action potential in both LQTS1 and LQTS2 cardiomyocytes (Figure 3a,b, Figure 4a,b, and Ext. Figure 7a–f). In addition, consistent with the effects of dextromethorphan on the potassium channels in TS cardiomyocytes, dextromethorphan treatment significantly increased both $I_{Kr}$ and $I_{Ks}$ currents in LQTS1 and LQTS2 cardiomyocytes (Figure 3c–f, Figure 4c–f, and Ext. Figure 7g,h). Mechanistically, similar to what was observed in TS cardiomyocytes (Figure 2j,k,n,o),

dextromethorphan treatment significantly reduced both SIGMAR1-hERG and SIGMAR1-$K_V7.1$ PLA signals in the LQTS1 and LQTS2 cardiomyocytes (Figure 3g–j and Figure 4g–j). Moreover, at the efficacious dose, dextromethorphan did not exhibit significant effects on the action potential in the corresponding isogenic control cardiomyocytes (Ext. Figure 6e–i, l–p), or on the voltage-dependent inactivation of $Ca_V1.2$ in LQTS1 and LQTS2 cardiomyocytes (Ext. Figure 7i–n). Furthermore, a significant increase in SIGMAR1 and ATF4 expression was detected in LQTS1 and LQTS2 cardiomyocytes, which may potentiate the cardiomyocytes to respond to dextromethorphan, while no significant changes in CDK5 and p35 expression were observed in LQTS1 and LQTS2 cardiomyocytes compared with control cardiomyocytes (Ext. Figure 7o–w). Overall, these results demonstrated that the SIGMAR1 agonist, dextromethorphan, increased $K^+$ currents in LQTS1 and LQTS2 cardiomyocytes through activating SIGMAR1 and that dextromethorphan treatment could be beneficial for LQTS1 and LQTS2 caused by trafficking mutations, which are more common forms of LQTS compared to TS.

## Effects of dextromethorphan on TS mouse model

Based on the intriguing *in vitro* results, we decided to move to *in vivo* study to examine the effect of dextromethorphan on TS further. We generated a cardiac-specific mouse model of TS, taking advantage of an inducible expression system using the *Rosa26* locus, a cardiac Cre driver (alpha-MHC/Myf6-MerCreMer), and a loxP pair with stop cassette in order to conditionally overexpress TS mutant channels in heart (Figure 5a)[37]. The inducible expression system allows us to express the mutant channels at the adult stage so as to avoid the heart developmental phenotypes that may lead to early lethality. A common challenge in the field of LQTS concerning murine models is the failure to recapitulate arrhythmic phenotypes *in vivo*[38] due to the fact that mice have different ion channel expression profiles and a remarkably higher heart rate compared to humans. Fortunately, our cardiac-specific mouse model of TS successfully recapitulated the LQTS phenotype and showed prolongation of QT interval at 4 days post tamoxifen administration, as revealed in electrocardiography (ECG) (Figure 5b–d). Next, we examined the effect of dextromethorphan on the LQTS phenotype by adding dextromethorphan to the drinking water for dosing. A low dose of quinidine was also added with dextromethorphan to improve the pharmacokinetic profile of dextromethorphan *in vivo* since quinidine is known to competitively inhibit the metabolism of dextromethorphan to dextrorphan. Clinically, a low dose of quinidine together with dextromethorphan is used to maintain a stable increase in the plasma concentration of dextromethorphan in humans[19,20]. To examine the pharmacokinetic profile of dextromethorphan with the dosing strategy, bloods were sampled from mice at different time point on day 4 and 11 to measure dextromethorphan concentration in plasma. The result indicated that the dosing strategy for dextromethorphan used in the study achieved a stable increase in plasma dextromethorphan level through the day (Ext. Figure 8a) with the plasma level of dextromethorphan in the dosed animals being comparable to the dextromethorphan level in human subjects taking 30 mg/day of dextromethorphan for 7 days (~10–60ng/ml)[19]. Next, we examined the effect of dextromethorphan on the LQTS phenotype in TS mice using ECG at day 4 and day 11. Dextromethorphan/quinidine significantly shortened the prolonged QT interval in TS mice at both time points (Figure 5c,d and Ext. Figure 8b,c). Moreover, dextromethorphan/quinidine did not significantly

affect the QT intervals in the control littermate mice (Figure 5c,d), which is consistent with clinical reports indicating no alternation of QT intervals in human subjects when used to treat pseudobulbar affect[19,20]. The overall results demonstrated that dextromethorphan not only rescued the phenotypes in TS iPSC-derived cardiomyocytes *in vitro* but also alleviated the LQTS phenotype in TS mice *in vivo*.

Lastly, to profile global changes in TS mouse hearts and the effects of dextromethorphan on the mutant hearts, we performed global proteomics analysis to profile protein expression changes in the hearts of controls, non-treated and dextromethorphan-treated TS mice at day 11. The proteomics results demonstrated that the expressions of many important molecules involved in cardiac excitation-contraction coupling, mitochondrial function, heart failure, fibrosis and cardiomyopathy such as Tmem38a/TRIC channel, Nppa/ANP, Postn/Periostin and Xirp2/Cmya3 (Cardiomyopathy-associated gene 3)[39–42] were altered in TS mouse hearts while dextromethorphan treatment restored the expression of these molecules to a comparable level as controls (Figure 5e and Ext. Figure 9). This supports the efficacy of dextromethorphan on TS hearts at endpoint, even though dextromethorphan treatment did not restore the expression of all the molecules involved in the pathways related to cardiac dysfunction and arrhythmias. In addition, interestingly, the proteomic analysis indicated that dextromethorphan treatment induced a significant increase in the expression of $K_V7.1$/Kcnq1 protein in TS hearts (Figure 5e and Ext. Figure 9), which is consistent with our observation using TS patient-specific iPSC-derived cardiomyocytes (Ext. Figure 5k–m). Because loss-of-function mutations in $K_V7.1$ are also known to cause LQTS1 and QT prolongation, we hypothesized that the increase in $K_V7.1$ expression might contribute to the beneficial effect of dextromethorphan on the prolonged QT interval in the TS mouse model. To validate the proteomic results, we examined the expression of $K_V7.1$ as well as the house-keeping molecules, ß-tubulin and Gapdh, using Western blotting and the mouse heart lysates. We found that, consistent with the proteomic results (Ext Figure 9), the expression of ß-tubulin significantly increased in TS mouse hearts compared with other groups while no changes in the expression of Gapdh proteins between the groups were observed (Ext. Figure 10a,b). We also found that, in line with the proteomics result and our observation using TS cardiomyocytes, there was a significant reduction in $K_V7.1$ protein expression in TS mouse hearts while dextromethorphan treatment restored the expression of $K_V7.1$ to a comparable level to control hearts (Ext. Figure 10a,c). When we examined the changes in *Kcnq1* transcripts in mouse hearts, dextromethorphan treatment did not significantly upregulate the transcription of *Kcnq1* in TS hearts although TS hearts showed a trend towards a reduction in *Kcnq1* gene expression compared with control hearts (Ext. Figure 10d). Overall, the results suggest that the significant reduction of $K_V7.1$ proteins in TS hearts may be associated with QT prolongation, although the contribution of $K_V7.1$ to cardiac action potential repolarization in rodents is known to be relatively smaller compared to humans, and dextromethorphan might alleviate the cardiac phenotypes in TS mouse model in part by increasing the expression of $K_V7.1$ in TS hearts through a post-transcriptional mechanism.

## Discussion

In summary, our results demonstrate that SIGMAR1 agonists such as dextromethorphan can rescue the phenotypes in TS iPSC-derived cardiomyocytes, TS mouse model as well

as LQTS1 and LQTS2 iPSC-derived cardiomyocytes with the G269S mutation in $K_V7.1$ channel and the A561V mutation in hERG channel, respectively. These results indicate that SIGMAR1 could be a therapeutic target for TS as well as LQTS1 and LQTS2 caused by trafficking mutations such as the G269S mutation in Kv7.1 channel and the A561V mutation in hERG channel. Furthermore, we explored the underlying mechanisms of the beneficial effects of SIGMAR1 activation on TS cardiomyocytes and found that SIGMAR1 may play a multi-faceted role in regulating $Ca_V1.2$ channel function in cardiomyocytes. First, SIGMAR1 directly interacted with CDK5 and SIGMAR1 activation induced a significant increase in the interaction and a significant reduction in CDK5 protein expression and activity in TS cardiomyocytes, which may restore the affected voltage-dependent inactivation of $Ca_V1.2$ in the patient cardiomyocytes through the mechanism that we proposed previously[6] and rescue the cellular phenotypes (Figure 1, Ext. Figure 1 and Ext. Figure 2). In addition, SIGMAR1 also directly interacts with $Ca_V1.2$ in TS cardiomyocytes and the activation of SIGMAR1 induced by dextromethorphan treatment modulated the interaction between SIGMAR1 and $Ca_V1.2$ (Ext. Figure 3h,i), which may also contribute to the beneficial effects of SIGMAR1 activation on TS cardiomyocytes. Our findings provided insights into the interactions between SIGMAR1, CDK5 and $Ca_V1.2$ in human iPSC-derived cardiomyocytes while the detailed molecular mechanisms concerning the interactions remained to be fully characterized. Moreover, it also merits to further investigate whether other players, such as calmodulin and calmodulin-dependent protein kinase II, which play important roles in regulating calcium channel function[43], or $Na^+/Ca^{2+}$ exchanger, which is known to modulate calcium homeostasis in cardiomyocytes[44], may interact with SIGMAR1 and mediate the effects of SIGMAR1 activation on calcium channel and ion homeostasis.

Unexpectedly, we found that there was a significant reduction in both $I_{Kr}$ and $I_{Ks}$ currents in TS cardiomyocytes compared to isogenic control cardiomyocytes (Ext. Figure 3j,k and Ext. Figure 5f), although our TS iPSC lines do not carry any mutations in hERG/*KCNH2* and $K_V7.1$/*KCNQ1* genes. More interestingly, we found that, in addition to its effects on $Ca_V1.2$ channel, the activation of SIGMAR1 by dextromethorphan also increased $K^+$ currents in TS cardiomyocytes (Figure 2, Ext. Figure 3 and Ext. Figure 5), which may further contribute to the normalization of action potential and restoration of ion homeostasis in TS cardiomyocytes. Mechanistically, it was observed that SIGMAR1 interacted with hERG and Kv7.1 channel in human iPSC-derived cardiomyocytes and dextromethorphan treatment modulated the interactions between SIGMAR1, hERG and $K_V7.1$ channel, increased the plasma-membrane localization of $K_V7.1$ and increased the gene and protein expression of $K_V7.1$ isoform 1 in TS cardiomyocytes. Although, to our knowledge, the interaction between SIGMAR1 and $K_V7.1$ has not been reported previously, the direct interaction between SIGMAR1 and hERG has been studied in leukemic cells, HEK cells and neonatal rat cardiomyocytes[12,32–34]. Our results confirmed the direct interaction between SIGMAR1 and hERG channel and SIGMAR1-mediated regulation of hERG channel function in human iPSC-derived cardiomyocytes while the detailed molecular mechanisms remain to be fully characterized. Additionally, dextromethorphan has been previously reported to inhibit hERG currents in a heterologous overexpression system[45] while we found that dextromethorphan treatment significantly increased hERG currents in human patient-specific iPSC-derived cardiomyocytes. There have been notable differences in the hERG currents in human iPSC-

derived cardiomyocytes[46] and heterologous systems potentially due to differences in cellular physiological conditions and associating molecules. Further investigations are needed to profile the effects and mechanisms of dextromethorphan and SIGMAR1 activation on hERG and $K_V7.1$ channels.

In contrast, when we examined the effects of dextromethorphan on the electrophysiological properties in isogenic control cardiomyocytes, no significant changes were observed in action potential (Figure 1), $Ca_V1.2$ inactivation (Ext. Figure 3) and $K^+$ currents (Ext. Figure 4) in the isogenic control cardiomyocytes treated with dextromethorphan at its efficacious dose on TS cardiomyocytes. We sought to understand the difference between the sensitivity of TS cardiomyocytes and isogenic control cardiomyocytes to the SIGMAR1 agonist dextromethorphan, and we found that at baseline there was a significant increase in the expression of SIGMAR1 transcripts and proteins in TS cardiomyocytes (Ext. Figure 2). Furthermore, we examined the expression of ATF4, a transcription factor that has been reported to directly regulate SIGMAR1 transcription[24], and observed an increase in ATF4 protein in TS cardiomyocytes, which may contribute to the increased expression of SIGMAR1 in TS cardiomyocytes. Overall, the results suggest that TS cardiomyocytes have an increased SIGMAR1 expression at baseline, which may predispose the cells to respond to SIGMAR1 agonists. In addition, it is also likely that, compared to TS cardiomyocytes with highly-disrupted ion homeostasis, normal cardiomyocytes without any mutations in cardiac ion channels have a higher capacity to tolerate moderate changes in ion channel function and maintain stable ion homeostasis, which contributes to the lack of changes observed in isogenic control cardiomyocytes with dextromethorphan treatment.

The data from TS cardiomyocytes encouraged us to test SIGMAR1 agonists on LQTS1 and LQTS2 cardiomyocytes with trafficking mutations. LQTS1 cardiomyocytes with the G269S trafficking mutation and LQTS2 cardiomyocytes with the A561V trafficking mutation have been reported to show decreased $K^+$ currents[35, 36], and we hypothesized that SIGMAR1 activation might be useful to restore $K^+$ currents and alleviate their cellular phenotypes. Consistent with our hypothesis, LQTS1 cardiomyocytes with the G269S mutation and LQTS2 cardiomyocytes with the A561V mutation did demonstrate a decrease in $K^+$ currents, and dextromethorphan treatment rescued the cellular phenotypes in the LQTS1 and LQTS2 cardiomyocytes (Figure 3, Figure 4 and Ext. Figure 6–7) through modulating the interactions between SIGMAR1, hERG and $K_V7.1$ channel and increasing $K^+$ currents. Our results demonstrated that SIGMAR1 activation could be beneficial for not only TS but also LQTS1 and LQTS2, which are caused by the G269S mutation in $K_V7.1$ channel and the A561V mutation in hERG channel, respectively. However, the effect of SIGMAR1 agonists and SIGMAR1 activation on LQTS1 and LQTS2 with other mutations remains to be investigated.

Intriguingly, in addition to TS human iPSC-derived cardiomyocytes, the SIGMAR1 agonist and FDA-approved cough suppressant dextromethorphan also exhibited beneficial effect on TS mouse model (Figure 5 and Ext. Figure 8–10). While dextromethorphan has been previously reported to have a protective effect on ouabain-induced acute arrhythmias[47], we reported that dextromethorphan treatment could be beneficial for a mouse model of the inherited cardiac arrhythmia, TS. One of the limitations of our study is that we did not

examine the effect of dextromethorphan on LQTS1 or LQTS2 mouse models due to the lack of LQTS1 or LQTS2 mouse model recapitulating arrhythmic phenotype *in vivo*[38], and additional studies are necessary to evaluate the potential effect of dextromethorphan on LQTS1 and LQTS2 *in vivo*. Furthermore, it is also worth noting that dextromethorphan has several limitations when it comes to clinical applications: dextromethorphan has a short half-life and induces nausea that may limit its tolerability and long-term usage, over-dose of dextromethorphan could potentially lead to severe adverse cardiac events[48,49] and the pharmacological profile of dextromethorphan in infants and young children are not fully investigated, which may comprise the main demographic of TS patients. Therefore, further investigations are absolutely required to evaluate whether dextromethorphan can be repurposed for alleviating cardiac arrhythmias in TS patients. In addition, TS is a multi-organ disorder that is featured by not only cardiac arrhythmias but also syndactyly, autism and hypoglycemia because of the important role of $Ca_V1.2$ channel in various organs[1,3,37,50]. Therefore, the effects of dextromethorphan on the dysfunction of other affected organs remain to be investigated.

In conclusion, although the role of SIGMAR1 has emerged in various diseases including neurological disorders and cancer[9–11] and more recently cardiovascular diseases[51,52] and COVID-19[53,54], our findings demonstrate that SIGMAR1 could be a therapeutic target for TS and potentially LQTS1 and LQTS2 caused by the G269S mutation in $K_V7.1$ channel and the A561V mutation in hERG channel, respectively. Further investigations are necessary to profile the global effects of SIGMAR1 activation and its agonists on different organs and tissues, and to develop and optimize SIGMAR1 agonists for future clinical applications.

## Method

### Ethical statement

All animal experimental procedures were carried out in accordance with regulations and established guidelines and were reviewed and approved by the Institutional Animal Care and Use Committee at Columbia University (#AC-AAAU2453).

### Human iPSC culture and cardiac differentiation

Timothy syndrome iPSC lines and their corresponding isogenic control iPSC lines were generated and reported previously[6,55]: Briefly, Timothy syndrome iPSC lines were generated with Lipofectamin LTX (Thermo Fisher Scientific) and the three episomal vectors (Addgene, #27077, 27078 and 27080) using skin fibroblasts isolated from Timothy syndrome patients. Their corresponding isogenic control iPSCs were generated using Lipofectamin LTX and plasmids of the transcription activator-like effector nuclease (TALEN) from the patient-specific iPSC lines, targeting *CACNA1C* gene (exon 8a). LQTS1 and LQTS2 iPSC lines were generated in Dr. Joseph Wu's lab at Stanford University and shared with us. The isogenic control iPSC lines were generated from the LQTS1 and LQTS2 iPSC lines using gene editing technology as reported in the current study. Human iPSCs were cultured with Essential 8 medium (Thermo Fisher Scientific) with 100 unit/ml penicillin and 100 μg/ml streptomycin (P.S.) on plates or dishes (Corning) coated with Geltrex (Thermo Fisher Scientific) following the manufacturer's instruction. Dispase

(Thermo Fisher Scientific) dissolved in the culture medium was used for cell dissociation/passaging. The iPSC lines were differentiated into cardiomyocytes following a monolayer-based protocol that we reported previously[55]. CHIR99021 (CHIR, GSK3 inhibitor, #1386, Axon MedChem, dose used for differentiation is titrated for each iPSC line and the dose range is 0.25–5 μM) and BIO (GSK3 inhibitor IX, #361550, Calbiochem), IWP-3 (Wnt inhibitor, #SML0533, Sigma-Aldrich) dissolved in Dimethyl Sulfoxide (DMSO, #276855, Sigma-Aldrich) were used for monolayer differentiation of iPSCs plated on Geltrex in 6-well plate or 10 cm dish. Only one freeze and thaw cycle was confirmed for all aliquots of compounds CHIR and BIO. Twice freeze and thaw cycle was confirmed for IWP-3 aliquots. For the differentiation protocol, DF20/5 media (DMEM/F-12 (with GlutaMax I) containing 20% or 5% Hyclone FBS, 1% MEM non-essential amino acids, P.S. and 0.1 mM 2-mercaptoethanol) was used for cardiac differentiation and culture. Additional D-glucose was added to only DF20 as high glucose media (final 4.5 g / l) to enhance mesoderm differentiation from Day 1 to Day 4. BIO (1μM) and CHIR (at the dose optimized for each line) treatment were conducted at day 2–4. The media with BIO and CHIR was changed every day. 2 μM IWP-3 treatment was conducted at day 5–11 and media was changed every other day. At day 5–7, DF20 media was used with IWP-3. DF5 media was used at day 7~ for IWP-3 treatment and maintenance, and the media was changed every other day. Changing media with small compounds required ~3 ml per well in 6-well and ~15 ml per 10 cm dish every other day since adding 2–2.5 ml of fresh media to a well of 6-well plates was not sufficient for high confluence of cells during differentiation into cardiomyocytes, resulting in lower efficiency of cardiac differentiation. Several lots of USDA-approved FBS (from Thermo Fisher, Hyclone and Gibco) were tested after we found that CHIR/BIO in DEME/F-12 worked with FBS, and HyClone FBS was only used for further monolayer differentiation since we found that this lot of Hyclone FBS provided slightly higher efficiency to generate cardiomyocytes reproducibly than other FBS.

## Gene editing to generate isogenic controls

A modification of a RNPs-based CRISPR/Cas9 editing protocol previously described[56] was used. Briefly, single strand guide RNA (sgRNA) and PAM sites were identified by using a freely available online tool (https://design.synthego.com/#/). Donors (ssODN) were designed manually following incorporation of desired nucleotide and silencing of the PAM sequence. Genecode release 26 (GRCh38.p10) was used as reference sequence for each target. Electroporation was performed using P3 Primary Cell 4D-Nucleofector X Kit S (Lonza, cat # V4XP-3032) and Lonza 4D nucleofector, as per manufacturer's instructions. RNP complex was prepared by adding 3ug of sgRNA (Integrated DNA Technologies, IDT) + 3ug ssODN (IDT) +2.5ug Cas9 protein (Alt-R S.p. HiFi Cas9 Nuclease V3, IDT) in P3 electroporation buffer. Solution was incubated for 30 minutes at room temperature to allow formation of RNP complex. Human iPSCs (LQTS1 and LQTS2 lines) were detached using warm Accutase (Stem Cell Technologies) and washed with $Ca^{2+}$/$Mg^{2+}$-free PBS, then $1\times10^6$ cells were resuspended in electroporation complex and electroporated using program CA150. Low density seeding ($3\times10^3$ cells/10cm dish) was performed to grow single cell colonies. Electroporated cells were allowed to grow for 48 h onto Matrigel (Corning)-coated 96-well plates with mTeSR Plus media (Stem Cell Technologies) supplemented with 10% Clone R (Stem Cell Technologies) at 37°C, 5% $CO_2$. Colonies were manually

picked in 96-well plates and genotyping was performed by genomic DNA isolation, PCR amplification of target region and subsequent Sanger sequencing (primers from Genewiz, Taq Polymerase from TaKaRa Bio). Edited clones were further expanded and tested for karyotypic abnormalities (Columbia University Genetics lab). sgRNA, ssODN and primer information are shown as below:

**KCNQ1—**sg RNA3: AGCCAGGTACACAAAGTACG PAM AGG

ssODN3:
GCCTAGGAGCTGATAACCACCCTGTACATCgGCTTCCTGGGCCTCATCTTCTC”g”T CGTACTTTGTGTACCTGGCTGAGAAGGACGCGGTGAACGAGTCA

g: target corrected A to g

“g”: PAM silence C to g

Primers: (PCR templet size: 560bp)

KCNQ1F1 GCTATATTGAAGCCGGCCCT amplification

KCNQ1R1 CCAGTGACCCCTCCGATTTC amplification

KCNQ1F2 CTTAGGCGTCTGCACAGGAG sequencing

**KCNH2—**sgRNA3: GCCTGCATCTGGTACGCCAT PAM CGG

ssODN3:
GTTCTTGCTCATGTGCACCTTTGCGCTCATCGcGCACTGGCTAGCCTGCATCTGGT ACGCCATCG”t”CAACATGGAGCAGCCACACATGGACTCACGCATCGGCT

c: target corrected T to C

“t”: PAM silence G to t

Primers: (PCR templet size: 388bp)

KCNH2F1 CAGTGTGGGCTTCACCTCTTAG amplification

KCNH2R1 TGCTGTTGTAGGGTTTGCCTATC amplification

KCNH2F2 GGATCTGACCTCTGATGCTCG sequencing

## Preparation of chemical compounds and biding modeling

Fluvoxamine maleate (F2802, Sigma-Aldrich), PRE-084 hydrochloride (Cat. No. 0589, TOCRIS), dextromethorphan (D2531, Sigma-Aldrich), NE-100 hydrochloride (Cat. No. 3133, TOCRIS) were dissolved in distilled water into stock solutions with a concentration of 10mM or 25mM. The stock solutions were stored in −80 °C and thawed only once for *in vitro* experiments. The putative binding of these agonists in SIGMAR1 was obtained using known templates in the SWISS-MODEL (Biozentrum) that produced a high identity with

human SIGMAR1 structure (5HK1 and 5HK2)[14]. This was used to generate docking models that were visualized using CueMol2.

## Patch clamp recording

Human iPSC-derived cardiomyocytes were dissociated into single cells for whole-cell patch clamp recordings at 1–2 months after cardiac differentiation was induced, and the dissociated cells were used for patch clamp recording 4–8 days after the dissociation, following a protocol reported previously[6]. Whole-cell patch-clamp recordings of iPSC-derived cardiomyocytes were conducted using a MultiClamp 700B patch-clamp amplifier (Molecular Devices) and an inverted microscope equipped with differential interface optics (Nikon, Ti-U). The glass pipettes were prepared using borosilicate glass (Sutter Instrument, BF150-110-10) using a micropipette puller (Sutter Instrument, Model P-97). Voltage-clamp measurements for voltage-dependent calcium channel inactivation were conducted using an extracellular solution consisting of 5mM $BaCl_2$, 160mM TEA and 10mM HEPES (pH7.4 at 25 °C) and a pipette solution of 125mM CsCl, 0.1mM $CaCl_2$, 10mM EGTA, 1mM $MgCl_2$, 4mM MgATP and 10mM HEPES (pH 7.4 with CsOH at 25 C). For calcium current recordings, instead another extracellular solution was used: 5mM $CaCl_2$, 137mM NMDG, 0.5 mM $MgCl_2$, 25mM CsCl, 10mM TEA-Cl, 10mM glucose and 10mM HEPES (pH 7.4 with CsOH at 25 °C). Cells were held at −90 mV and then at −50 mV (2-sec hold), stimulated with pulses from −60 to +20 for the current-voltage relationship of the $Ba^{2+}$ currents. The recordings were conducted under room temperature. Voltage-clamp recording for $I_{Kr}$ measurements was conducted in normal Tyrode's solution containing 140 mM NaCl, 5.4 mM KCl, 1 mM $MgCl_2$, 10 mM glucose, 1.8 mM $CaCl_2$ and 10 mM HEPES (pH 7.4 with NaOH) at 37 °C supplemented with 0.5 μM nisoldipine ($I_{Ca}$ current blocker, Sigma-Aldrich, N0165) and 5 μM (−)-[*3R, 4S*]-chromanol-293B ($I_{Ks}$ current blocker, TOCRIS, #1475) using the pipette solution 120 mM K d-gluconate, 25 mM KCl, 4 mM MgATP, 2 mM NaGTP, 4 mM $Na_2$-phospho-creatine, 10 mM EGTA, 1 mM $CaCl_2$ and 10 mM HEPES (pH 7.4 with KCl at 25 °C). The following pulse protocol was used: 2-s voltage clamp applied from −10 mV to 50mV (Δ10mV, holding at −40 mV, 0.1 Hz, at 37 °C). All of the components used for above recording solutions were purchased from Sigma-Aldrich except (−)-[*3R, 4S*]-chromanol-293B (TOCRIS). After recordings, the extracellular solution was switched to one containing 1 μM E-4031 (TOCRIS, #1808) using perfusion. E-4031-sensitive current was measured and analyzed as $I_{Kr}$ current using Clampfit 10.4 (Axon Instruments). For $I_{Ks}$ current recordings, instead of (−)-[*3R, 4S*]-chromanol-293B, E-4031 (0.5 μM) was used for base recordings and then (−)-[*3R, 4S*]-chromanol-293B (10 μM) was applied to measure (−)-[*3R, 4S*]-chromanol-293B-sensitive currents as $I_{Ks}$. The recordings were conducted at 37 °C.

Current-clamp recordings were conducted in normal Tyrode solution containing 140mM NaCl, 5.4mM KCl, 1mM $MgCl_2$, 10mM glucose, 1.8mM $CaCl_2$ and 10mM HEPES (pH7.4 with NaOH at 25°C) using the pipette solution: 120mM K D-gluconate, 25mM KCl, 4mM MgATP, 2mM NaGTP, 4mM Na2-phospho-creatin, 10mM EGTA, 1mM $CaCl_2$ and 10mM HEPES (pH 7.4 with KCl at 25°C). The recordings were conducted at 37 °C. Cardiac action potentials were stimulated (2ms, 1nA, 0.2 Hz for Timothy syndrome lines or 0.5 Hz for the other lines) in current clamp mode at 37 °C. Recorded action potentials were analyzed using

Clampfit 10.4. Control recordings were obtained from cardiomyocytes without treatment. The after treatment recordings were obtained from cardiomyocytes that had been treated with either dextromethorphan, fluvoxamine or PRE-084 at the dose of 5μM for 2 hours in the cardiomyocyte culture media that we reported previously[6,55]. The dose of 5μM was empirically chosen for the compounds based on our previous studies. The patch clamp data was acquired and analyzed using pClamp 10 (Molecular Devices) and Clampfit 10.4 (Axon Instruments).

## Cardiomyocyte contraction analysis

The working solution of the SIGMAR1 agonist PRE-084 was made by diluting the stock solution in cardiomyocyte media to a final concentration of 5 μM PRE-084. The contraction analysis was performed as reported previously[5,6]. In brief, images were collected at a rate of 5 frames per second using the NIS-elements software (4.51.01, Nikon) and converted to multi-frame TIFF images for analysis using the NIS-elements viewer. The multiple-frame TIFF images were processed using the Image Processing Toolbox in MATLAB R2009b (Mathworks). Relative motion between successive frames was quantified by subtracting each frame from the preceding frame and summing across all pixels. Movement was calculated by plotting the relative motion over time. Contractions were detected as a peak of relative motion and a second, typically smaller peak, corresponded to the relaxation of the cardiomyocytes. Peaks were selected manually and the rate of contraction was measured. The length of time between contractions was also measured and contraction irregularity was measured by calculating the ratio of the standard deviation to the mean of the intervals between contractions. The Timothy syndrome cardiomyocytes were used for the tests at day 21–22 after cardiac differentiation. The movies were taken before the treatment, and 2 hours after the treatment of PRE-084 from the intact monolayer Timothy syndrome cardiomyocytes. The cardiomyocytes from two Timothy syndrome iPSC lines (clone#: TS1-E3-5 & TS2-E7-1) were used for this contraction assay. The contraction rate and the irregularity of each sample before and after treatment were compared using paired two-tailed Student's *t*-test. The contraction rate and irregularity value of each sample after treatment were normalized to its respective value before treatment in the corresponding figures.

## Calcium imaging

For the calcium transient recordings to confirm the phenotype in Timothy syndrome cardiomyocytes compared with control cardiomyocytes and examine the effects of dextromethorphan on the abnormal spontaneous calcium transients in Timothy syndrome cardiomyocytes, the cardiomyocytes were prepared with the same experimental schedule as described in electrophysiology method section. The Nikon automatic microscope (Nikon Eclipse TiE with a motorized stage) connected to sCMOS camera (Andor Zyla sCMOS 4.2 MP) together with a stage top incubator (at 37°C, 5% $CO_2$ and 20% $O_2$, controlled by TOKAI HIT Hypoxia gas delivery system) were used for this experiment. Nikon objective lens 40x (Nikon CFI Plan Apo Lambda, NA 0.95) was used for single cell recordings and the cardiomyocyte culture media was used as bath solution. The cells were infected with AAV9-GCaMP6f (UPenn Vector Core/Addgene) within a week of when calcium imaging was performed. For the testing of dextromethorphan, a basal recording was acquired from

each cell before the treatment of dextromethorphan and after the basal recording, the solution was changed to cardiomyocyte culture media with 5 μM dextromethorphan or water. The recordings were then measured every thirty minutes for two hours after the treatment of dextromethorphan from the same cells. The calcium transient frequency and the calcium transient half (50%) decay time from the recordings before and after treatment were analyzed. The values of each parameter after treatment were normalized to the baseline values acquired before treatment for data presentation in the corresponding figures.

### *in vitro* CDK5 activity assay

To examine the endogenous CDK5 activity, a CDK5 activity assay was conducted following the protocol that we reported previously[6]. Human iPSC-derived cardiomyocytes differentiated from Timothy syndrome iPSCs were collected at day 26 or day 27 for the assay. For the compound-treated groups, the cardiomyocytes were treated with PRE-084 at the dose of 5μM for two hours before being collected for the assay. Cardiomyocytes were isolated from monolayer culture and lysed with the cell lysis buffer containing 1% NP-40, 20mM Tris-HCl, 137mM NaCl, 1x protease inhibitor cocktail, 1x phosphatase inhibitor cocktail 3 (Sigma-Aldrich, # P0044) and 1x phosphatase inhibitor cocktail (Sigma-Aldrich, # P8340), pH 7.4. The protein concentration in the samples was measured using a standard bicinchoninic acid (BCA) assay kit (Piers/Thermo Fisher Scientific). 40 μg of proteins from each sample were aliquoted and used as one sample for CDK5 immunoprecipitation. The sample was incubated with CDK5 antibody-conjugated agarose beads (CDK5 (J-3) AC, Santa Cruz Biotechnology, #:sc-6247 AC) for 2 hours at 4°C (rocking continuously) for CDK5 immunoprecipitation. 5μl resuspended bead solution was used for the immunoprecipitation of CDK5 from each sample. After immunoprecipitation, the beads were washed three times with cold Tris-buffered saline (TBS) and twice with room temperature TBS. A reaction mix containing 1X Reaction Buffer A, 50 μM DTT, 50 μM ATP, 1 μg Histone H1 in distilled water was added to each sample for detecting CDK5 activity. The stock of PHA-793887 (Selleckchem) was diluted with DMSO and added to the corresponding samples in the PHA-793887 treated Timothy syndrome groups at the concentration of 5 μM. The same volume of DMSO was added to the rest of the samples to achieve the same concentration of DMSO in all the reactions. A series of samples for a standard curve were prepared based on the manufacturer's instructions to determine the ATP-ADP conversion from the luminescence signals in every round of experiment. The kinase reaction tubes with the reaction mixes were incubated at 26–27°C for 60 minutes for the kinase reaction. The ADP-GloTM reagent (Promega) was then added to the reactions for an incubation of 40 minutes at 26–27°C to deplete the ATP in the reactions. Next the detection reagent was added to the reactions for an incubation of 45 minutes at 26–27°C. 20μl of the sample from each tube was then transferred into a 96 well microplate and the luminescence was measured with the GloMax® 96 Microplate Luminometer (1.9.2. Promega) with an integration time of 1.5s. The luminescence values were converted into the ATP-ADP conversion values based on the standard curve. Four rounds of experiment were conducted. The values from each round of experiments were normalized to the average value of the Timothy syndrome cardiomyocyte samples without PHA-793887 addition before being pooled together for the final analysis that is showed in Ext. Figure 1b.

### Western blotting of human cardiomyocytes

Anti-CDK5R1/p35 (Rabbit polyclonal Ab, Catalog # sc-820 “discontinued”, Clone # C-19, 1: 1,000 dilution, Santa Cruz; Rabbit recombinant monoclonal Ab, Catalog # C64B10, 1:500 dilution, Cell Signaling Technology), anti-CDK5 antibody (Mouse monoclonal Ab, Catalog # MABS50, Clone # 1H3 “discontinued”, 1:1,000 dilution, Millipore; Rabbit recombinant monoclonal Ab, Catalog # ab40773, 1:2,000 dilution, Abcam), anti-SIGMAR1 (Rabbit polyclonal Ab, Catalog # 42–3300, 1:1,000 dilution, Thermo Fisher Scientific), anti-ATF4 (Rabbit recombinant monoclonal Ab, Catalog # ab184909, 1:500 dilution, Abcam), anti-GAPDH (Rabbit recombinant monoclonal Ab, Catalog # ab181602, 1:10,000 dilution, Abcam) and anti-beta-Tubulin antibody (Mouse monoclonal Ab, Catalog # T5201, Clone # TUB 2.1, 1:8,000 dilution, Sigma-Aldrich) were used for Western blotting. Some of the Timothy syndrome cardiomyocytes were treated with 5 μM PRE-084 in cardiomyocyte culture media for two hours before being collected for Western blotting. The Timothy syndrome cardiomyocytes from the same round of differentiation were collected as control. The cells were isolated from the monolayer and lysed with the cell lysis buffer containing 1% Triton X-100, 50mM Tris-HCl, 150mM NaCl, 250mM sucrose, 1x protease inhibitor cocktail, 1x phosphatase inhibitor cocktail 3 and 1x phosphatase inhibitor cocktail, pH 7.4. The concentration of total proteins in each sample was measured using BCA assay kit. Next, 20 μg of proteins from each sample were aliquoted and denatured with the sample buffer containing Urea and being boiled for 5 minutes at 95 °C. The samples were loaded to the Tris-HCl based SDS-PAGE gels with 5% stacking gel and 10% separation gel along with the ladder (Pre-stained SDS-PAGE standards, broad range, catalog # 161–0318, Biorad). The proteins were electro-transferred to PVDF-membranes (InvitrolonTM PVDF, Catalog # LC2005, NOVEX/Thermo Fisher Scientific) using the XCell SureLockTM Mini-Cell system (Thermo Fisher Scientific) overnight at 4 °C. Next day, the membranes were blocked with the SuperBlock Blocking Buffer in PBS (phosphate-buffered saline, Thermo Fisher Scientific, # 27515) for 30 minutes at room temperature and then incubated with the primary antibody (diluted in the SuperBlock Blocking buffer) overnight, followed by an incubation of the corresponding secondary antibody (Pierce/Thermo Fisher Scientific, anti-mouse # 31430; anti-rabbit, #31460,1:8,000 dilution in the SuperBlock Blocking buffer) for 30 minutes at room temperature. The membranes were then incubated with the Pierce ECL Western blotting substrate (Thermo Fisher Scientific, # 32209) followed by exposing to X-ray films (CL-X posureTM film, Thermo Fisher Scientific, # 34091) in a dark room. For sequential immunoblotting, the membranes were stripped with the stripping buffer containing 62.5mM Tris-HCl, 2% SDS, 114mM 2-mercaptoethanol at 42°C for 15–20 minutes, and washed six times with PBS. The stripped membranes were then re-blocked with SuperBlock Blocking Buffer for the next immunoblotting. For the immunoblotting of beta-tubulin, the membrane was stripped, re-blocked with the SuperBlock Blocking Buffer and incubated with the beta-tubulin antibody at room temperature for 30 minutes. The rest of the steps were the same. The Western blot analysis to examine p35 protein expression in Timothy syndrome cardiomyocytes before and after 5 μM PRE-084 treatment was repeated six times with independent samples from different rounds of differentiation for validation. The Western blot analysis to examine CDK5 expression in Timothy syndrome cardiomyocytes before and after 5 μM PRE-084 treatment was repeated four times using samples from different rounds of differentiation for validation. Western blot band intensities

were quantified using Image J and the values were normalized to the corresponding beta-tubulin band intensities or GAPDH band intensities. The values from Timothy syndrome cardiomyocytes two hours after the treatment of 5 μM PRE-084 were normalized to the values from Timothy syndrome cardiomyocytes without treatment for the presentation in the corresponding figure. The values from LQTS1/LQTS2/Timothy syndrome cardiomyocytes were normalized to the values from control cardiomyocytes for the presentation in the corresponding figures. The blotting images (uncropped, with the molecular markers) are also shown in Supplementary Figure.

## Immunocytochemistry

Proximity ligation assay was conducted using Sigma-Aldrich Duolink Kit (DUO92101/DUO92103). Human iPSC-derived cardiomyocytes were treated with 5μM dextromethorphan for 2 hours at 37°C and then washed with PBS. Next, the samples were fixed in a 4% PFA/2% sucrose solution for 15 min at room temperature, washed three times with PBS and permeabilized for 10 minutes at room temperature with 0.2% Triton X-100. The permeabilized samples were then washed three times with PBS and blocked for one hour at 37 °C in a humidity chamber using the blocking solution from the Duolink kit. The samples were next incubated in primary antibody overnight at 4°C (KCNQ1/$K_V$7.1, Alomone lab, # APC-022, 1:500; SIGMAR1, Santa Cruz, # sc-137075 (mouse), 1:500; SIGMAR1, Abcam, # ab53852 (rabbit), 1:500; KCNH2/hERG, Santa Cruz, # sc-377388, 1:500; CDK5, Abcam, # ab40773, 1:500; $Ca_V$1.2, Alomone labs, # ACC-003, 1:100). The remainder of the procedure was done following the Sigma Aldrich PLA fluorescence detection protocol. Cell fluorescent images were taken using a confocal microscope (Nikon, A1RMP) and the Epi-fluorescent microscopies, which were used for the above physiological recordings. PLA signal quantifications were conducted blindly: M.Y. coded the image files and R.B and A.D.K. analyzed the signals using ImageJ-win64 (Fiji) in a blinded manner. For immunostaining, the cells were fixed and stained using Wheat Germ Agglutinin (WGA, Alexa Fluor™ 647 conjugated, Thermo Fisher Scientific, # W34266, 5μg/ml). Next the cells were permeabilized and stained with hERG (Alomone lab, # APC-062, 1:200) or Kv7.1 antibody (Alomone lab, # APC-022, 1:200) followed by the corresponding secondary antibody and mounted with mounting medium containing DAPI (from the above Duolink Kit, Sigma-Aldrich). Quantifications of WGA-hERG or WGA-Kv7.1 co-localization were conducted blindly: R.B. coded the image files and L.S. analyzed the images using ImageJ-win64 (Fiji) and quantified the fraction of green over red signals in a blinded manner. R.B. analyzed the values using GraphPad Prism (version 7.0).

## Quantitative RT–PCR

RNA from control cardiomyocytes, Timothy syndrome cardiomyocytes without treatment and two hours after the treatment of 5 μM PRE-084 was prepared using the RNeasy Mini kit and RNase-Free DNase set (Qiagen). Mouse heart tissue RNA samples were also prepared using the same method. cDNA was synthesized using the SuperScript III First-Strand Synthesis System for RT–PCR (Thermo Fisher Scientific). The cDNA (21 μl) was diluted with DNase-free water (Thermo Fisher Scientific) at 1:1 and 1 μl of the samples was used for quantitative RT-PCR (qPCR) analysis. SYBR Advantage qPCR Premix (Clontech/TaKaRa Bio) and StepOnePlus real time PCR systems (Thermo Fisher Scientific) with

StepOne software (version 2.3, Life Technologies) were used for qPCR. The primer sets for detecting the hCDK5, hSIGMAR1, mKcnq1 and hGAPDH/mGapdh transcripts (h, human; m, mouse) were as follows: hCDK5 Forward 5'- GGCTTCAGGTCCCTGTGTAG-3', Reverse 5'- ATGGTGACCTCGATCCTGAG-3'; hSIGMAR1 Forward 5'- GGGAGACGGTAGTACACGG-3', Reverse 5'- AGGAGCGAAGAGTATAGAAGAGG-3'; hGAPDH, Forward 5'- GATGACATCAAGAAGGTGGTGA-3', Reverse 5'- GTCTACATGGCAACTGTGAGGA-3'; mKcnq1 Forward 5'- CTTGTGGTGTTCTTTGGGACA – 3', Reverse 5' - CCCAGATGCCCACGTACTT - 3'; mGapdh Forward 5' - CTTCACCACCATGGAGAAGG – 3', Reverse 5' - TGAAGTCGCAGGAGACAACC – 3'. Two independent Timothy syndrome iPSC lines (TS1-E3-5, $n$=6; TS2-E7-1, $n$=3) and two paired isogenic control lines (TS1-E3-5c3-14, $n$=3; TS2-E7-1c6, $n$=3 / ref. 6) as well as two independent normal subject-derived iPSC lines (IM-E1-5, $n$=3; NH-E1-1, $n$=3) were used for the quantitative RT-PCR (Ext. Figure 2i). Timothy syndrome iPSC-derived cardiomyocytes (TS1-E3-5, $n$=4 independent differentiation) with and without dextromethorphan treatment were used with hGAPDH (ver 2), Forward 5'- CTCACCGGATGCACCAATGTT -3', Reverse 5'- CGCGTTGCTCACAATGTTCAT -3'; hKCNQ1 (isoform 1), Forward 5'- GCGTCTCCATCTACAGCACG -3', Reverse 5'- GAAGTGGTAAACGAAGCATTTCC-3'; hKCNQ1 (isoform 2), Forward 5'- GACTTCCTCATCGTCCTGGT-3', Reverse 5'-GAAGAACACCACCAGCACGA-3'; hERG/KCNH2, Forward 5'- TTCGACCTGCTCATCTTCGG -3', Reverse 5'- CGATGCGTGAGTCCATGTGT -3' (Ext. Figure 5l,m). Following the manufacturer's instruction, human normal cardiomyocytes (FUJIFILM, iCell, #11713) were transfected using ViaFect (Promega) and hATF4 plasmid that was made from LV-SD (CAG promoter, Addgene, #12105, LV-Cre-SD, no longer available currently, Cre was removed by using EcoRI-XhoI sites). Human ATF4 DNA fragment was synthesized (IDT, gBlock) and subcloned to LV-SD vector. High transfection efficiency (~70%) in human cardiomyocytes was confirmed using yellow fluorescent protein (YFP) plasmid. hATF4, Forward 5'- CCCTTCACCTTCTTACAACCTC -3', Reverse 5'- TGCCCAGCTCTAAACTAAAGGA -3'; hSIGMAR1 (ver 2), Forward 5'- CGAAGAGATAGCGCAGTTGG -3', Reverse 5'- TCCACGATCAGACGAGAGAAG -3' were used with the above hGAPDH primer set (ver 2) for the ATF4-transfected cardiomyocytes (Ext. Figure 2o,p). The transfected cells were also used for Western blotting using hSIGMAR1 antibody (Ext. Figure 2q,r). The above primer sets were synthesized by Eton Bioscience or IDT. The CT value of each sample at 50% of the amplification curve was used and GAPDH/Gapdh was used to normalize the expression of target molecules.

## Mouse electrocardiography

Conditional mouse model of Timothy Syndrome was generated by M.Y., targeting the *Rosa26* locus with a G406R mutant in the calcium channel *Cacna1c* gene[37] (Figure 5a). αMHC-MerCreMer transgenic mice (Myh6-cre/Esr1, JAX #5657) were used for this mouse study. When αMHC-MerCreMer transgenic mice are bred with Timothy syndrome mice containing loxP-flanked sequences, tamoxifen-inducible Cre-mediated recombination is expected to result in deletion of the floxed sequences in the heart cells of the offspring to specifically overexpress Timothy syndrome mutant channels in the hearts. The mice

were maintained using standard diet under 12-h light/dark cycle. Subcutaneous 4-lead electrocardiograms of isoflurane-anesthetized adult mice (backcrossed with C57BL/6, Envigo, # 044, 12-week old female) were performed using emka ECG and recorded using iox 2.8.0.19 (emka TECHNOLOGIES). Recordings were conducted a day 4 and 11 after tamoxifen (Sigma-Aldrich, 50μg/B.W.(g)/day/mouse, *i.e.,* approximately 1mg/day/mouse) was administrated at day 1–3. Dextromethorphan/quinidine (Sigma-Aldrich, # Q0875; ratio, dextromethorphan: quinidine = 2:1) was dissolved in drinking water for dosing. RR and QT intervals were measured manually using ecgAUTO v2.8.1.27 (emka TECHNOLOGIES), Microsoft Excel for Mac 2011 (Microsoft) and Prism 6/7 software (GraphPad). To evaluate the pharmacokinetic profile of dextromethorphan with the designed dosing strategy in mice, we conducted a pharmacokinetic analysis. 12-week old C57BL/6 female mice were used for the analysis and were dosed in the same way as the ECG experiments. Blood was sampled from the dosed animals at 8am, noon and 8pm on day 4 and 11 after treatment and collected through the tail vein using a heparinized microhematocrit capillary tube (Fisher Scientific, # 22-362566). Plasma was isolated by centrifugation and transferred to a 1.5 mL clear Eppendorf tube (Eppendorf, # 22364120) containing 5μL of 0.5M EDTA (Thermo Fisher Scientific, # 15575020), and stored at −80 °C until further analysis. The plasma concentration of dextromethorphan from dosed animals was measured and analyzed at Columbia University Biomarkers Core Laboratory using a validated customized Liquid Chromatography Mass Spectrometry (Agilent 6410A mass spectrometer coupled with an Agilent 1290 Infinity UHPLC) based assay.

## Global quantitative proteomics by mass spectrometry

For global quantitative proteomics of mouse ventricular heart samples (the above day-11 mouse), tandem mass tag (TMT)-based quantitative proteomics was used. In brief, frozen mouse ventricular heart were lysed by bead-beating in 9M urea and 200mM EPPS (pH 8.5), supplemented with protease and phosphatase inhibitors. Samples were reduced with 5mM TCEP and alkylated with 10mM iodoacetamide (IAA) that was quenched with 10mM DTT. A total of 400μg of protein was chloroform–methanol precipitated. Protein was reconstituted in 200mM EPPS (pH 8.5) and digested by Lys-C overnight and trypsin for 6h, both at a 1:50 protease-to-peptide ratio. Digested peptides were quantified using a Nanodrop at 280nm and 200 μg of peptide from each sample were labeled with 800 μg TMT reagent using 11-plex TMT kit[57]. TMT labels were checked, 0.5μg of each sample was pooled, desalted and analyzed by short SPS-MS3 method, and using normalization factor, samples were bulk mixed at 1:1 across all channels and bulk mixed samples were fractionated using the Pierce™ High pH Reversed-Phase Peptide Fractionation Kit (Thermo Fisher Scientific) and each fraction was dried down in a speed-vac. Dried peptides were dissolved in 10 μl of 3% acetonitrile/0.1% formic acid injected using SPS-MS3. The UltiMate™ 3000 RSLCnano system (Thermo Scientific) and EASY Spray™ source (Thermo Fisher Scientific) with Acclaim™ PepMap™100 2 cm × 75 μm trap column (Thermo Fisher Scientific) and EASY-Spray™ PepMap™ RSLC C18. 50 cm × 75 μm ID column (Thermo Fisher Scientific) were used to separate fractioned peptides with a 5–30% acetonitrile gradient in 0.1% formic acid over 127min at a flow rate of 250nL/min. After each gradient, the column was washed with 90% buffer B for 5min and re-equilibrated with 98% buffer A (0.1% formic acid, 100% HPLC-grade water) for 40min. For BPRP-separated proteome fractions,

the full MS spectra were acquired in the Orbitrap Fusion™ Tribrid™ Mass Spectrometer (Thermo Fisher Scientific) at a resolution of 120,000. The 10 most intense MS1 ions were selected for MS2 analysis. The isolation width was set at 0.7 Da and isolated precursors were fragmented by CID at a normalized collision energy (NCE) of 35% and analyzed in the ion trap using “turbo” scan speed. Following acquisition of each MS2 spectrum, a synchronous precursor selection (SPS) MS3 scan was collected on the top 10 most intense ions in the MS2 spectrum. SPS-MS3 precursors were fragmented by higher energy collision-induced dissociation (HCD) at an NCE of 65% and analyzed using the Orbitrap. Raw mass spectrometric data were analyzed using Proteome Discoverer 2.2 to perform database search and TMT reporter ions quantification. TMT tags on lysine residues and peptide N termini (+229.163 Da) and the carbamidomethylation of cysteine residues (+57.021 Da) was set as static modifications, while the oxidation of methionine residues (+15.995 Da), deamidation (+0.984) on asparagine and glutamine and phosphorylation (+79.966) on serine, threonine, and tyrosine were set as a variable modification. Data were searched against a UniProt mouse with peptide-spectrum match (PSMs) and protein-level at 1% FDR. The signal-to-noise (S/N) measurements of each protein were normalized so that the sum of the signal for all proteins in each channel was equivalent to account for equal protein loading. Results obtained from PD2.2 were further analyzed using Perseus statistical package[58] is part of the MaxQuant distribution. Significantly changed protein abundance was determined by ANOVA with $P<0.05$ (permutation-based FDR correction). Pathway analysis was performed using ingenuity IPA.

### Western blotting for $K^+$ channels

For the Western blot analysis of mouse tissue samples, remaining mouse tissue from the proteomic analysis was used and further resuspended in a solution containing 9M urea, 50mM Ammonium bicarbonate, protease and phosphatase inhibitors. Protein concentrations were determined using a standard BCA assay. 30ug of protein of each sample were aliquoted and denatured in a urea sample buffer and boiled for 5 minutes at 95°C. The samples were loaded into the Tris-HCl based SDS-Page gels for electrophoresis and electro-transferred to PVDF-membranes using the XCell SureLockTM Mini-Cell system overnight. The next day the samples were placed in blocking solution (5% skim milk in TBS) overnight at 4 °C. The following day the membranes were incubated with the primary antibody solution overnight at 4 °C (KCNQ1/$K_V$7.1 antibody, Alomone lab, # APC-022, 1:2,000 dilution; GAPDH antibody, Abcam, Catalog # ab181602, 1:10,000 dilution; beta-tubulin antibody, Sigma Aldrich, T5201, 1:8,000 dilution). Membranes were then incubated in the corresponding secondary antibody for one hour at room temperature and then developed with Pierce ECL Western blotting substrate followed by exposure to X-ray films in a dark room. The blotting images (uncropped, with the molecular markers) are also shown in Supplementary Figure. For the Western blotting for $K^+$ channels in human iPSC cardiomyocytes, some of the Timothy syndrome cardiomyocytes were treated with 5 μM dextromethorphan in cardiomyocyte culture media for two hours before being collected for Western blotting. The Timothy syndrome cardiomyocytes from the same round of differentiation were collected as control. KCNH2/hERG antibody (Santa Cruz, F-12, # sc-377388, 1:500 dilution) and the same/above KCNQ1/Kv7.1 antibody and were used for the samples (Ext. Figure 5d,k). The cells were lysed in 1x cell lysis buffer (Cell Signaling Technology, # 9083) containing 1x

protease inhibitor cocktail, 1x phosphatase inhibitor cocktail 3 (Sigma-Aldrich, # P0044,) with 1x phosphatase inhibitor cocktail (Sigma-Aldrich, # P8340,). After which, the samples were proceeded and analyzed using the same procedure as the mouse tissues.

## Data availability

Source datasets including global proteomics (Figure 5e and Ext. Figure 9) are available in the Source Data file.

## Statistics and reproducibility

The statistics used for every figure have been indicated in the corresponding figure legends. The Student's *t*-test (paired and unpaired) was conducted with the *t*-test functions in Microsoft Excel software. The Student's *t*-test was two-tailed. The one-way ANOVA with Tukey's, Sidak's, Bonferroni's or Dunnett's post-hoc multiple comparison analysis was conducted with the GraphPad Prism 6/7 software. All the data meet the assumptions of the statistical tests. All the samples used in this study were biological repeats, not technical repeats. All experiments were conducted using at least two independent experimental materials/cohorts to reproduce similar results. No samples were excluded from the analysis in this study, except one outlier (defined by Grubbs' test) in the analysis for plasma dextromethorphan concentrations (Ext. Figure 8a). All the graphs in the figures, except the plasma concentration of dextromethorphan in Ext. Figure 8a, are mean ± s.d.. Ext. Figure 8a is mean ± s.e.m.

## Extended Data

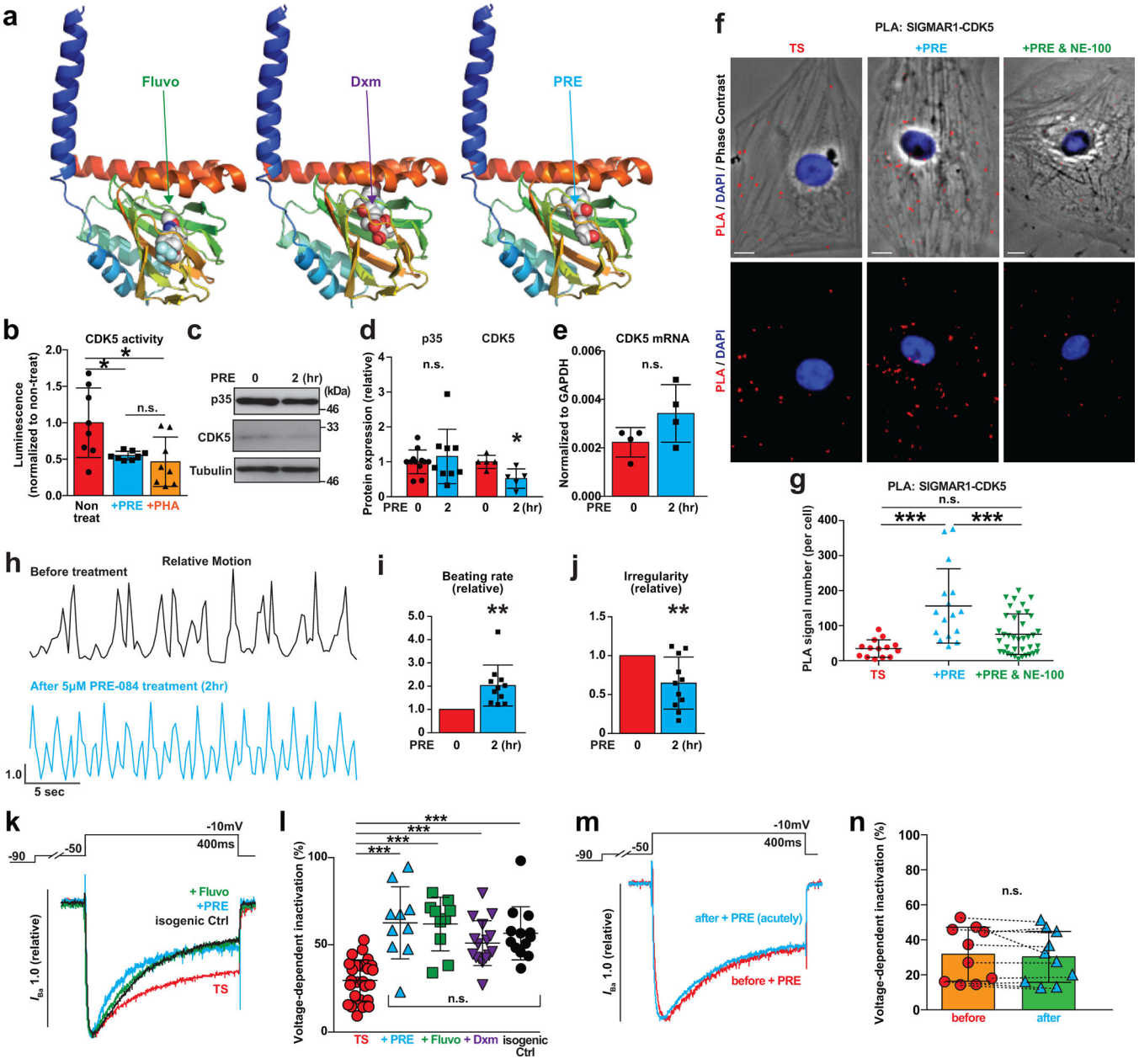


**Extended Data Figure 1 |. The effect of SIGMAR1 agonists on CDK5, contraction and calcium channel in Timothy syndrome iPSC-derived cardiomyocytes.**

(**a**) Docking models of SIGMAR1-Fluvo, -Dxm and -PRE. (**b**) PRE-084 (5μM, 2hr) reduced CDK5 kinase activity in Timothy syndrome (TS) cardiomyocytes. PHA-793887 (PHA, 5μM), a CDK5 inhibitor, was used as positive control for the assay ($n$=8/group). (**c-e**) The effects of PRE (5μM, 2hr) on CDK5R1/p35 protein (**c, d,** $n$=12 for baseline and $n$=9 for 2 hr after treatment) and CDK5 protein (**c, d,** $n$=5/group) and mRNA (**e,** $n$=4/group). (**f**) Representative epi-fluorescent and phase-contrast images of TS cardiomyocytes without treatment, with PRE-084 (+PRE, 5μM, 2hr) or PRE-084 and NE-100 treatment

(+PRE & NE-100, both 5μM, 2hr) from proximity ligation assay (PLA, SIGMAR1-CDK5, red, DAPI, blue). Scale bar, 10μm. (**g**) SIGMAR1-CDK5 PLA quantification in PRE-treated ($n$=16), PRE&NE-100-treated ($n$=38) and non-treated TS cardiomyocytes ($n$=14). (**h**) Representative traces of relative motion analysis of TS cardiomyocyte contractions before (black) and after 2-hr PRE-084 treatment (blue). The representative traces were obtained from Supplementary Movie 1 and 2. (**i-j**) Relative changes of beating rate (**i**) and irregularity (**j**) ($n$=11) of TS cardiomyocytes after PRE-084 treatment. (**k**) Representative traces of $Ba^{2+}$ currents in TS cardiomyocytes without treatment or treated with PRE-084 (+PRE), or fluvoxamine (+Fluvo) (each, 5μM, 2hr) and in isogenic control cardiomyocytes (Ctrl). +Dxm representative trace is shown in Figure 2f. (**l**) Voltage-dependent calcium channel inactivation was significantly enhanced by PRE ($n$=10), Fluvo ($n$=10) and Dxm ($n$=16) treatment in TS cardiomyocytes compared to non-treated cells ($n$=25). n.s., no significant differences between +PRE, +Fluvo, +Dxm and isogenic Ctrl groups ($n$=13). (**m**) Representative traces of $Ba^{2+}$ currents in TS cardiomyocytes before treatment and acutely treated with PRE (5μM, ~5–10 mins). (**n**) Voltage-dependent calcium channel inactivation was not significantly changed by acute PRE treatment in TS cardiomyocytes ($n$=10). All data are mean ± s.d. One-way *ANOVA* with Tukey's multiple comparisons was used for b, g and One-way *ANOVA* with Sidak's multiple comparisons was used for l. Paired two-tailed Student's $t$-test was used for i, j, n, and unpaired two-tailed Student's $t$-test was used for d, e. *$P$<0.05, ** $P$<0.01, *** $P$<0.001, n.s., not significant. Cell samples from at least two independent differentiations were used.

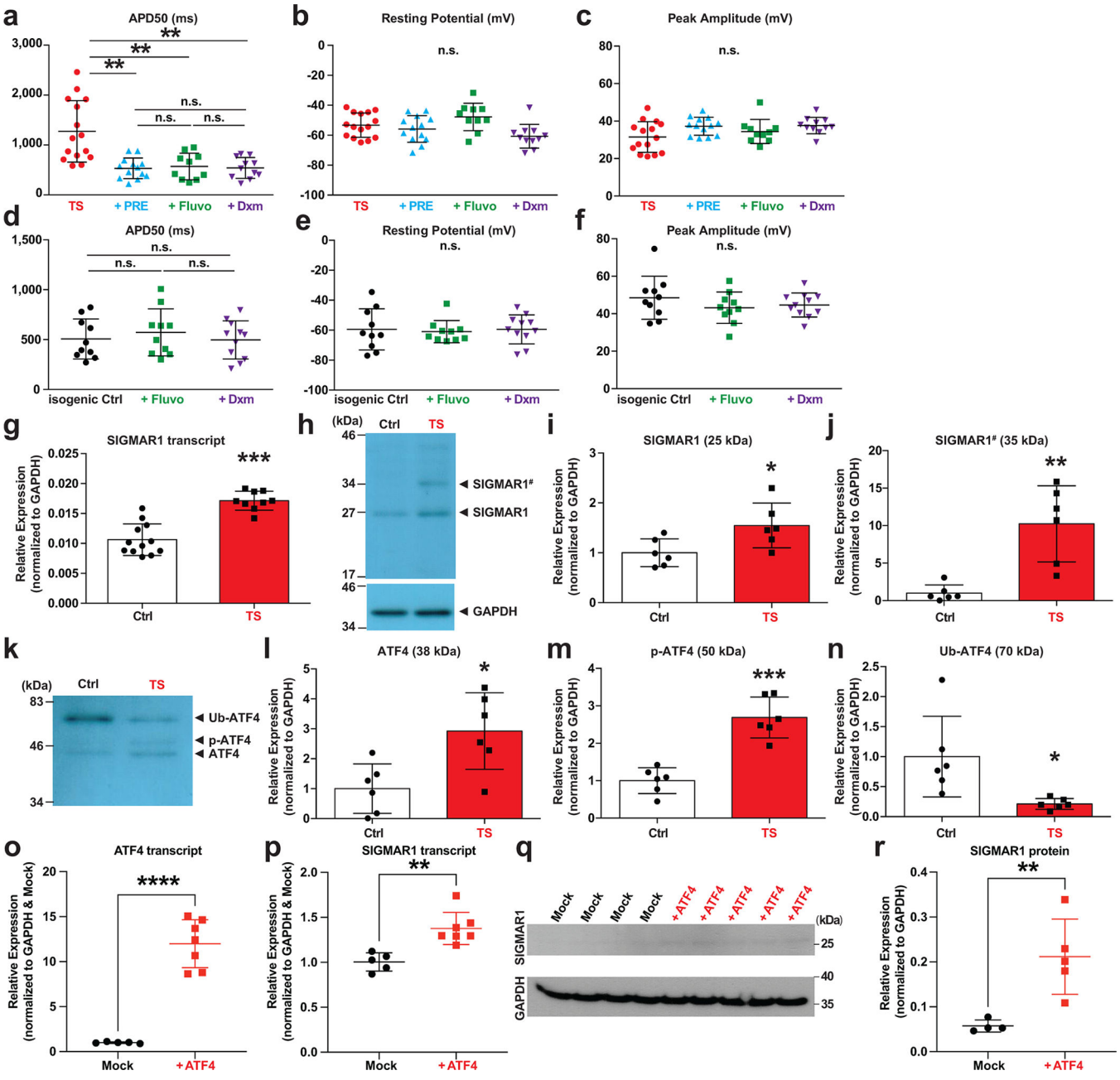


**Extended Data Figure 2 |. The effect of SIGMAR1 agonists on action potential and SIGMAR1 and ATF4 expression profiling in Timothy syndrome iPSC-derived cardiomyocytes.**

(**a-c**) Action potential parameters, APD50 (**a**), resting potential (**b**) and peak amplitude (**c**) in Timothy syndrome (TS) cardiomyocytes without treatment ($n$=15) or treated for 2 hrs with 5μM SIGMAR1 agonists, PRE-084 (+PRE, $n$=13), fluvoxamine (+Fluvo, $n$=10) or dextromethorphan (+Dxm, $n$=11). APD90 is shown in Figure 1d. (**d-f**) Action potential parameters, APD50 (**d**), resting potential (**e**) and peak amplitude (**f**) in isogenic control (Ctrl) cardiomyocytes without treatment ($n$=10) and treated for 2 hrs with 5μM SIGMAR1 agonists, Fluvo ($n$=10) or Dxm ($n$=11). (**g**) Quantification of human SIGMAR1 transcripts (normalized to GAPDH) in Timothy syndrome ($n$=9 from two independent lines) and

control cardiomyocytes ($n$=12 from four independent lines). (**h**) Representative immunoblots of human SIGMAR1 and GAPDH protein using lysates from TS and control iPSC-derived cardiomyocytes. (**i-j**) Quantification of SIGMAR1 25kDa protein band (**i**) and 35kDa protein expression (**j**, normalized to GAPDH) in TS iPSC-derived cardiomyocytes compared to the isogenic Ctrl ($n$=6/group). The molecular weight of SIGMAR1 is ~25 kDa while the 35kDa band (#) has been reported previously and might be a dimer of a full-length SIGMAR1 with a SIGMAR1 splice variant[59]. (**k**) Representative immunoblots of human ATF4 using the same lysates from TS and isogenic Ctrl iPSC-derived cardiomyocytes shown in Ext. Figure 2h. (**l-n**) Quantification of ATF4 38kDa protein band (**l**, non-modified), 50kDa (**m**, phosphorylated) and 70kDa protein expression (**n**, ubiquitinated, normalized to GAPDH) in TS iPSC-derived cardiomyocytes compared to the isogenic Ctrl ($n$=6/group). (**o-r**) ATF4 overexpression (**o**) significantly increased SIGMAR1 transcription (**p**) and protein expression (**q,r**) in normal human cardiomyocytes transfected with ATF4 plasmid (+ ATF4, o&p, $n$=7, r, $n$=5). The cardiomyocytes were harvested 24 hr after the lipofection. The empty vector was used as a negative control (Mock, o&p, $n$=5, r, $n$=4). (**q**) Representative immunoblots of human SIGMAR1 and GAPDH using the lysate from the transfected cardiomyocytes. All data are mean ± s.d. One-way *ANOVA* with Tukey's multiple comparisons was used for a-f and unpaired two-tailed Student's $t$-test was used for g, i, j, l, m, n, o, p, r. * $P$<0.05, ** $P$<0.01, *** $P$<0.001, **** $P$<0.0001, n.s., not significant. Cell samples from at least two independent differentiations were used.

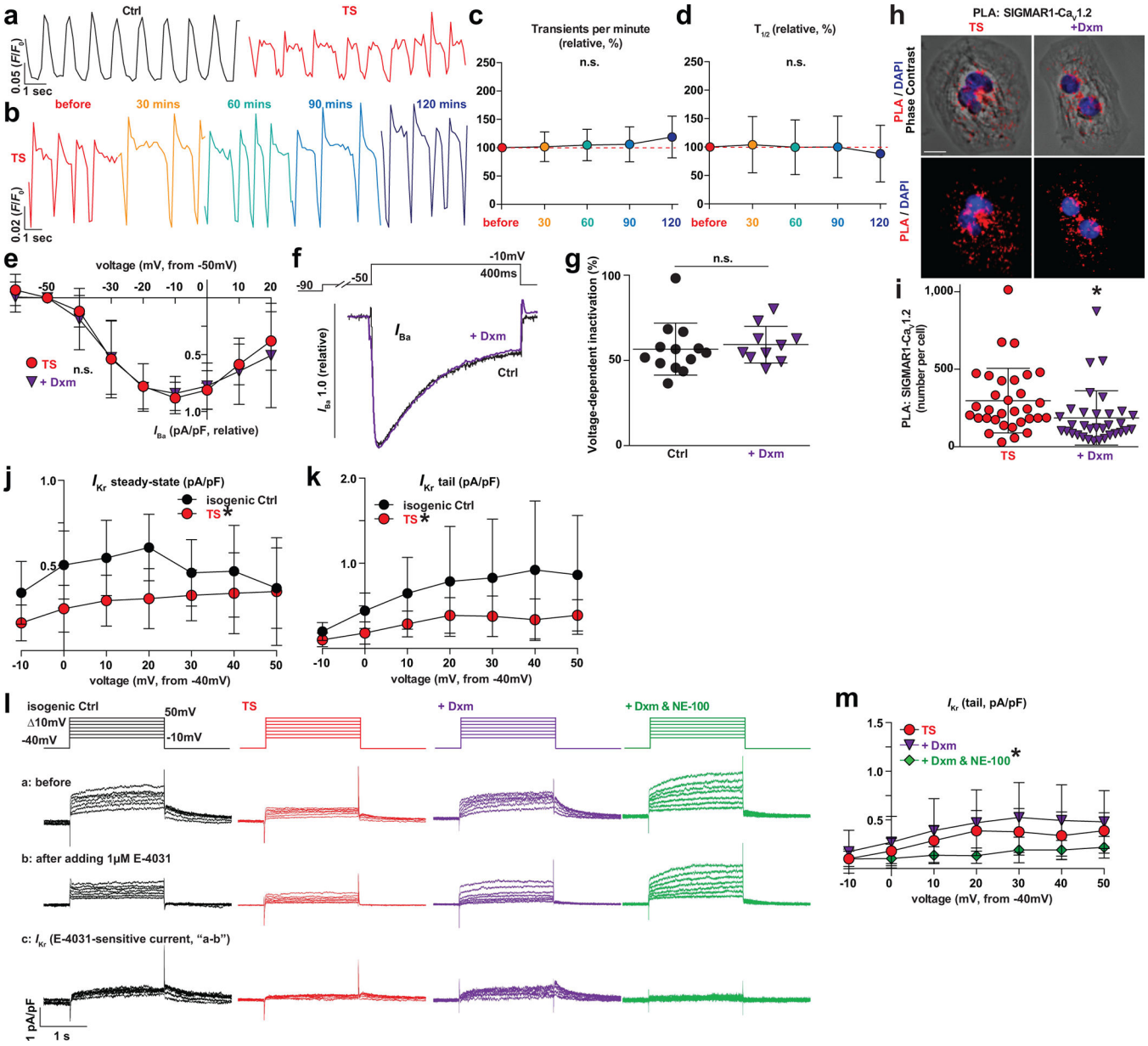


**Extended Data Figure 3 |. The effect of dextromethorphan on cardiac calcium and hERG channels in Timothy syndrome iPSC-derived cardiomyocytes.**

(**a-b**) Representative traces of time-course calcium imaging in spontaneously contracting isogenic control (Ctrl, black) and Timothy syndrome (TS, red) cardiomyocytes. (**c-d**) Calcium transient frequency (**c**) and duration (**d**) analysis in TS cardiomyocytes during the 2-hr imaging ($n$=32). (**e**) Current-voltage relationship of $Ba^{2+}$ recordings in Dxm-treated ($n$=12) and non-treated TS cardiomyocytes ($n$=13). (**f**) Representative traces of $Ba^{2+}$ currents in isogenic control cardiomyocytes without treatment (Ctrl) or treated with dextromethorphan (+Dxm). (**g**) Voltage-dependent calcium channel inactivation was not altered by Dxm ($n$=10) in the isogenic control cardiomyocytes compared to non-treated cells ($n$=13). (**h**) Representative epi-fluorescent and phase-contrast images of TS cardiomyocytes without and with Dxm (+Dxm) from proximity ligation assay (PLA, SIGMAR1-$Ca_V1.2$,

red, DAPI, blue). Scale bar, 10μm. (**i**) SIGMAR1-$Ca_V1.2$ PLA quantification in Dxm-treated ($n$=33) and non-treated TS cardiomyocytes (TS, $n$=32). (**j**) $I_{Kr}$ current steady-state amplitudes were significantly reduced in TS cardiomyocytes ($n$=10) compared to isogenic control ($n$=10) at −10, 0 and 10 mV steps from −40mV hold. (**k**) $I_{Kr}$ tail currents were significantly reduced in TS cardiomyocytes ($n$=10) compared to isogenic control ($n$=10) at −10, 0, 10 and 20 mV steps. (**l**) Representative traces of $I_{Kr}$ currents (E-4031-sensitive) in isogenic Ctrl cardiomyocytes (black) and TS cardiomyocytes treated with Dxm (purple), Dxm & NE-100 (green) or without treatment (red, TS). The $I_{Kr}$ traces are shown in Figure 2h. (**m**) There was no significant difference in $I_{Kr}$ current (tail) between Dxm-treated ($n$=9) and non-treated TS cardiomyocytes ($n$=10) while Dxm & NE-100 ($n$=10) significantly reduced tail currents compared to Dxm at 10, 20, 30, 40 and 50 mV steps and also to non-treated TS at 20mV step from −40mV hold. All data are mean ± s.d. The treatment of Dxm or NE-100 for all experiments was 5μM, 2hrs. One-way *ANOVA* with Tukey's multiple comparisons was used for c, d between the time points to before and used for m at each voltage step. Unpaired two-tailed Student's *t*-test were used for g, i between the groups and used for e, j, k at each voltage step. * $P$<0.05, n.s., no significant. The samples were from at least two independent differentiations.

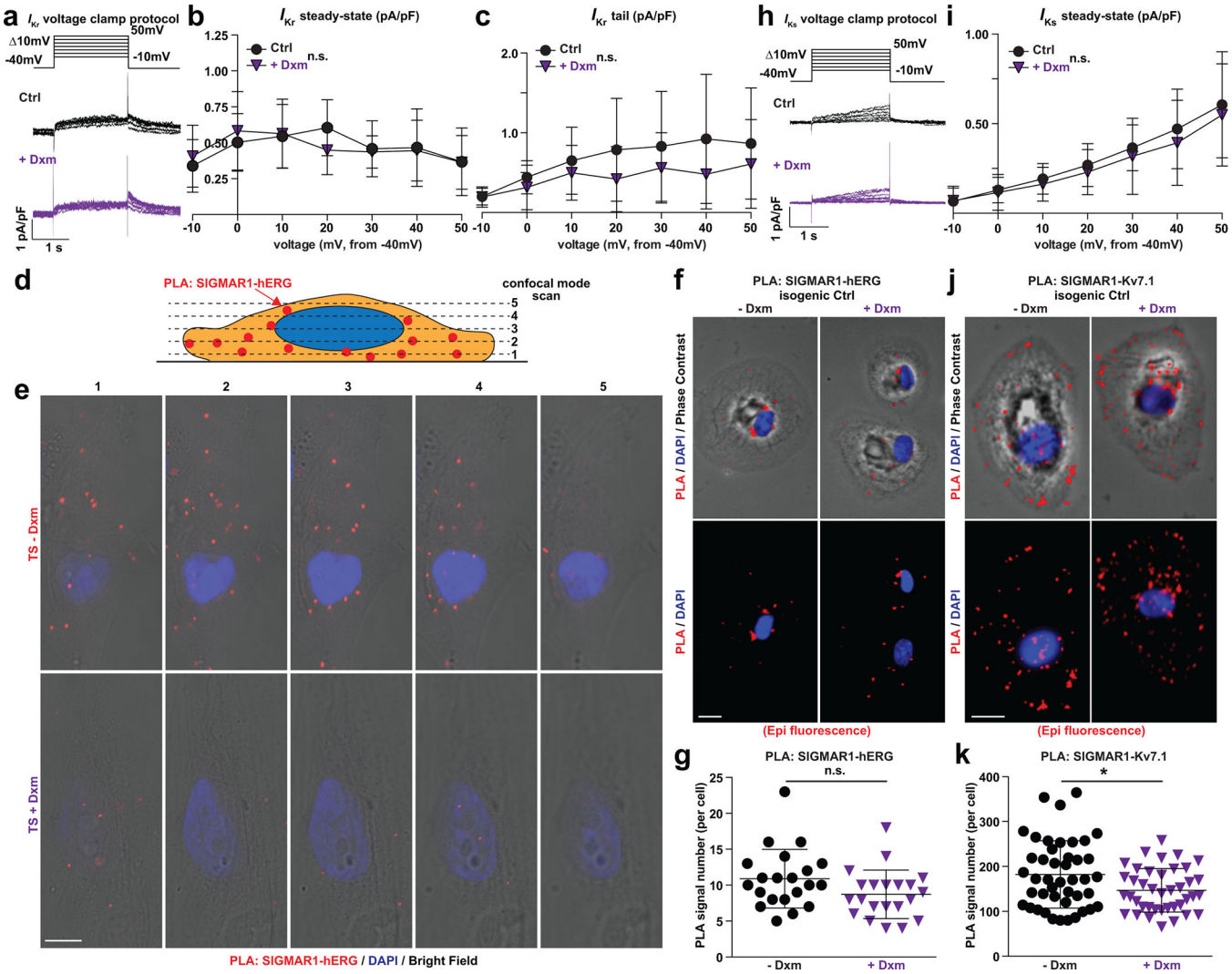


**Extended Data Figure 4 |. The effect of dextromethorphan on potassium channels in human cardiomyocytes derived from isogenic control iPSCs.**

(**a**) Representative traces of $I_{Kr}$ current (E-4031-sensitive) in isogenic control (Ctrl) cardiomyocytes treated with Dxm (5μM, 2hr) or without treatment. (**b-c**) $I_{Kr}$ current amplitude (**b**) and tail $I_{Kr}$ current (**c**) were not significantly changed by Dxm in the isogenic Ctrl cardiomyocytes ($n$=10/group). (**d**) Schematic representation of confocal imaging for proximity ligation assay (PLA, SIGMAR1-hERG, red) in human iPSC-derived cardiomyocytes. (**e**) Representative confocal fluorescent images of TS cardiomyocytes used for PLA (SIGMAR1-hERG, red) and DAPI (blue) staining. Dxm treatment (+Dxm, 5μM, 2hr) was conducted to examine the effect of Dxm on PLA signals in TS cardiomyocytes. #3 images are used in Figure 2j. Scale bar, 10μm. (**f**) Representative epi-fluorescent and phase-contrast images of isogenic Ctrl cardiomyocytes used for PLA (red, SIGMAR1-hERG) and DAPI (blue) staining. Dxm treatment (+Dxm, 5μM, 2hr) was conducted to examine the effect of Dxm on PLA signals in the cardiomyocytes. Scale bar, 10μm. (**g**) Quantification of PLA signal number of SIGMAR1-hERG in Dxm-treated ($n$=21) and non-treated ($n$=21) isogenic Ctrl cardiomyocytes. (**h**) Representative traces of $I_{Ks}$ current (Chromanol 293B-

sensitive) in isogenic control (Ctrl) cardiomyocytes treated with Dxm or without treatment. (**i**) $I_{Ks}$ current amplitude analysis in the isogenic Ctrl cardiomyocytes with Dxm (5μM, 2hr, $n$=9) or without treatment ($n$=10). (**j**) Representative epi-fluorescent and phase-contrast images of isogenic Ctrl cardiomyocytes used for PLA (red, SIGMAR1-$K_V$7.1) and DAPI (blue) staining. Dxm treatment (+Dxm, 5μM, 2hr) was conducted to examine the effect of Dxm on PLA signals in the cardiomyocytes. Scale bar, 10μm. (**k**) Quantification of PLA signal number of SIGMAR1-$K_V$7.1 in Dxm-treated ($n$=40) and non-treated ($n$=44) isogenic Ctrl cardiomyocytes. All data are mean ± s.d. Unpaired two-tailed Student $t$-test was used for g,k between the groups, and for b,c,i at each voltage step. * $P$<0.05. n.s., not significant. The cell samples were from at least two independent differentiations.

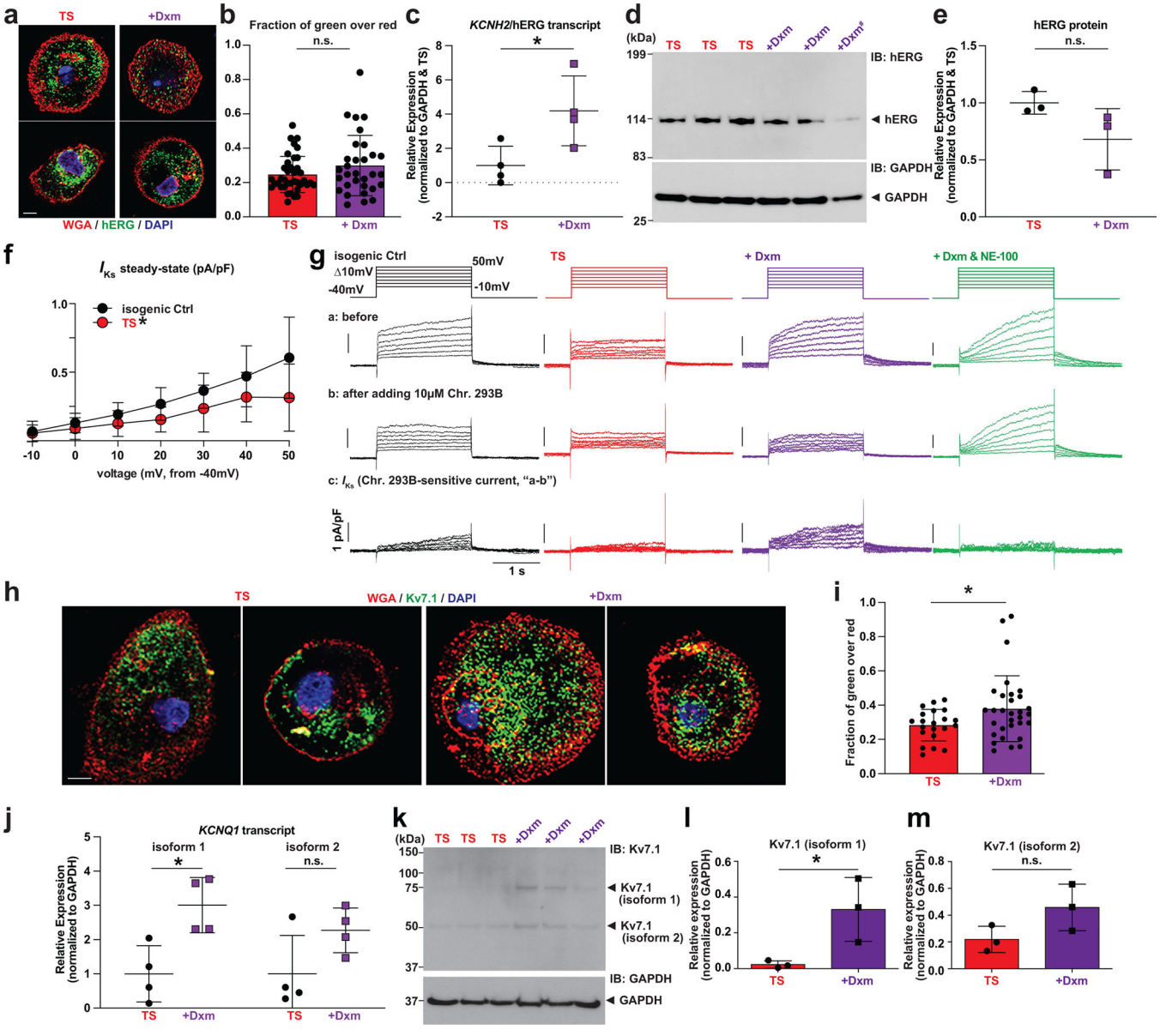


**Extended Data Figure 5 |. The effect of dextromethorphan on potassium channels in Timothy syndrome iPSC-derived cardiomyocytes.**

(**a**) Representative confocal fluorescent images of Timothy syndrome cardiomyocytes without treatment (left, TS) and with dextromethorphan (+Dxm). Scale bar, 5μm. (**b**) Quantification of fraction of green (hERG) over red (WGA) fluorescence signals in TS cardiomyocytes without treatment ($n$=38) and with Dxm ($n$=31). (**c**) Quantification of *KCNH2* transcript in TS cardiomyocytes with and without Dxm ($n$=4/group). (**d**) Representative immunoblots of human hERG and GAPDH protein using lysates from non-treated and Dxm-treated TS cardiomyocytes. (**e**) Quantification of hERG protein expressions (normalized to GAPDH) in non-treated and Dxm-treated TS cardiomyocytes ($n$=3/group). The trend towards a decreased hERG protein expression in the treated group might be driven by one sample ($^{\#}$) with a reduced loading amount compared with others. (**f**) $I_{Ks}$ current steady-state amplitudes were significantly reduced in TS cardiomyocytes ($n$=10) compared to isogenic control ($n$=10) at 20 and 50 mV steps from −40mV hold. (**g**) Representative traces of $I_{Ks}$ currents (Chromanol 293B-sensitive) in isogenic Ctrl cardiomyocytes (black) and TS cardiomyocytes treated with Dxm (purple), Dxm and NE-100 (green) or without treatment (red, TS). The $I_{Ks}$ traces are shown in Figure 2l. (**h**) Representative confocal fluorescent images of Timothy syndrome cardiomyocyte without treatment (left, TS) and treated with dextromethorphan (+Dxm). Scale bar, 5μm. (**i**) Quantification of fraction of green ($K_V$7.1) over red (WGA) fluorescence signals in TS cardiomyocytes without treatment ($n$=21) and treated with Dxm ($n$=31). (**j**) Quantification of *KCNQ1* transcripts (isoform 1 and 2) in TS cardiomyocytes without treatment and treated with Dxm ($n$=4/group). (**k**) Representative immunoblots of human $K_V$7.1 and GAPDH protein using lysates from non-treated and Dxm-treated TS cardiomyocytes. (**l-m**) Quantification of $K_V$7.1 isoform 1 (**l**) and isoform 2 protein expressions (**m**, normalized to GAPDH) in non-treated and Dxm-treated TS cardiomyocytes ($n$=3/group). All data are mean ± s.d. The treatment of Dxm or NE-100 for all experiments was 5μM, 2hrs. Unpaired two-tailed Student's $t$-test was used for b, c, e, i, j, l, m between the groups and used for f at each voltage step. * $P$<0.05. n.s., not significant. The cell samples were from at least two independent differentiations.

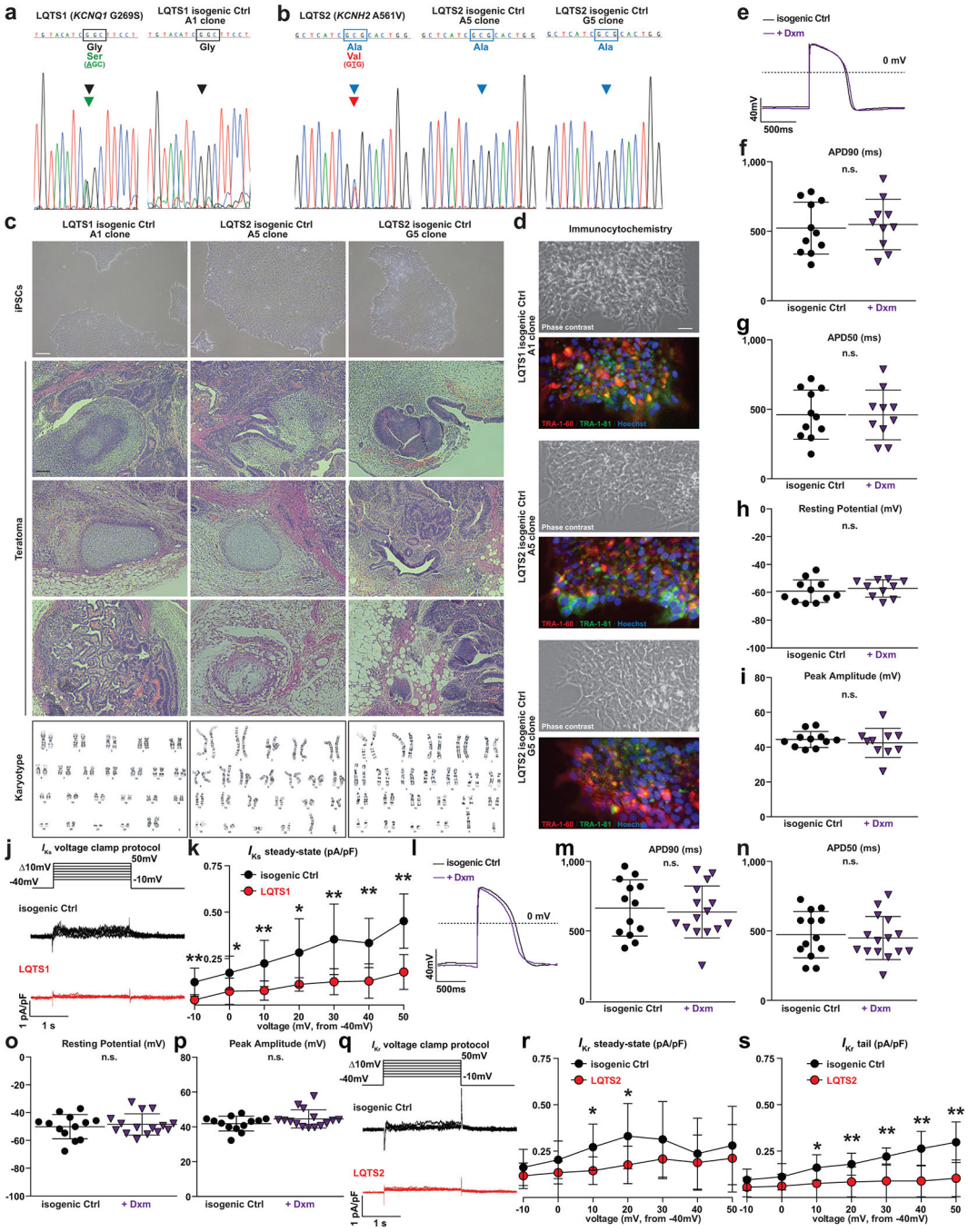


**Extended Data Figure 6 |. Generation of isogenic controls from long QT syndrome type 1 and 2 iPSCs.**

(**a-b**) Sequencing results confirmed the successful generation of isogenic control (Ctrl) iPSC lines from long QT syndrome type 1 (**a**) and type 2 (**b**). (**c**) Characterization of the isogenic Ctrl iPSC lines (top, phase contrast image; middle, teratoma formation assay). Scale bar, 200μm. The isogenic Ctrl iPSC demonstrated normal karyotype (bottom). (**d**) Representative images of TRA-1-60 (red)/TRA-1-81 (green)/Hoechst (nuclei, blue) stain in isogenic Ctrl iPSC lines. Scale bar, 20μm. (**e**) Representative traces of 0.5Hz-paced action

potentials in LQTS1 patient-specific isogenic Ctrl iPSC-derived cardiomyocytes without treatment or treated with Dxm. (**f-i**) Analysis of action potential parameters, APD90 (**f**), APD50 (**g**), resting potential (**h**) and peak amplitude (**i**), in isogenic Ctrl cardiomyocytes without treatment ($n$=11) or treated with Dxm ($n$=10). (**j**) Representative traces of $I_{Ks}$ currents (Chromanol-293B-sensitive) in long QT syndrome type 1 (LQTS1) patient-specific cardiomyocytes and the isogenic Ctrl cardiomyocytes. (**k**) $I_{Ks}$ current steady-state amplitudes were significantly reduced in LQTS1 cardiomyocytes ($n$=10) compared to the isogenic control ($n$=11) at all voltage steps from −40mV hold. (**l**) Representative traces of 0.5Hz-paced action potentials in long QT syndrome type 2 (LQTS2) patient-specific isogenic Ctrl iPSC-derived cardiomyocytes without treatment or treated with Dxm. (**m-p**) analysis of action potential parameters, APD90 (**m**), APD50 (**n**), resting potential (**o**) and peak amplitude (**p**), in the isogenic Ctrl cardiomyocytes without treatment ($n$=13) or treated with Dxm ($n$=15). (**q**) Representative traces of $I_{Kr}$ currents (E4031-sensitive) in LQTS2 patient-specific cardiomyocytes and the isogenic Ctrl cardiomyocytes. (**r**) $I_{Kr}$ current steady-state amplitudes were significantly reduced in LQTS2 cardiomyocytes ($n$=10) compared to the isogenic control ($n$=12) at 10 and 20 mV steps from −40mV hold. (**s**) $I_{Kr}$ tail currents were significantly reduced in LQTS2 cardiomyocytes compared to the isogenic control at 10, 20, 30, 40 and 50 mV steps from −40mV hold. All data are mean ± s.d. The treatment of Dxm for the experiments was 5μM, 2hrs. Unpaired two-tailed Student's $t$-test were used for f, g, h, i, m, n, o, p between the groups and for k, r, s at each voltage step. * $P$<0.05, ** $P$<0.01, n.s., not significant. The cardiomyocytes were from at least two independent differentiations.

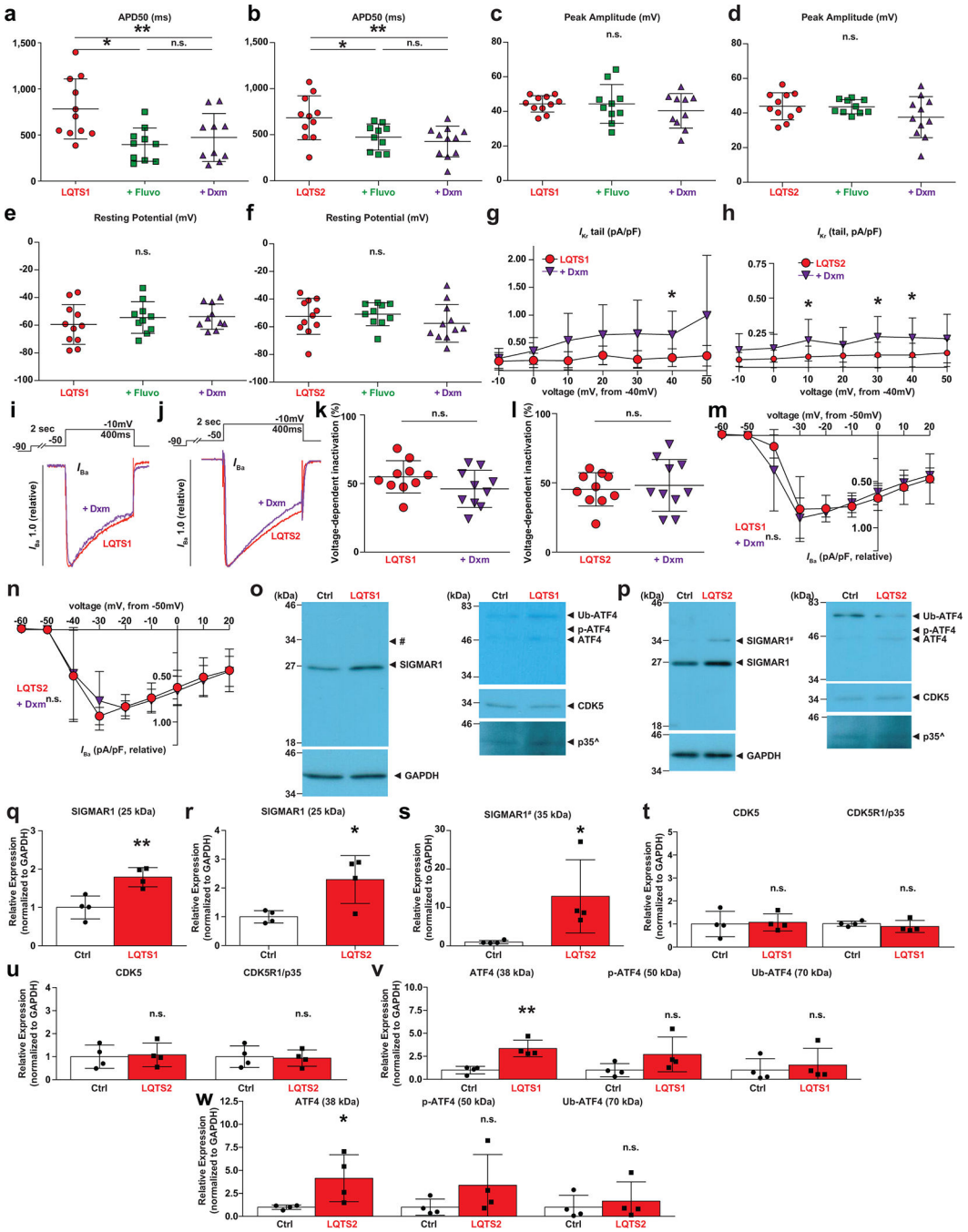


**Extended Data Figure 7 |. The effect of dextromethorphan on the phenotypes in long QT syndrome type 1 and type 2.**

(**a-f**) Analysis of APD50 (50% from peak, **a, b**), peak amplitude (**c, d**) and resting potential (**e, f**) in LQTS1 cardiomyocytes without treatment ($n$=11) or treated with fluvoxamine (Fluvo, $n$=10) or dextromethorphan (Dxm, $n$=10) and in LQTS2 cardiomyocytes without treatment ($n$=11) or treated with Fluvo ($n$=10) or Dxm ($n$=11). (**g,h**) $I_{Kr}$ current (tail) was significantly increased by Dxm in LQTS1 cardiomyocytes at 40mV step (**g,** LQTS1, $n$=10; +Dxm, $n$=9) and in LQTS2 cardiomyocytes at 10, 30 and 40mV

steps (**h,** LQTS2, *n*=10; +Dxm, *n*=9). (**i,j**) Representative traces of $Ba^{2+}$ currents in LQTS1 (**i**) or LQTS2 cardiomyocytes(**j**) without treatment or treated with Dxm. (**k,l**) Voltage-dependent calcium channel inactivation was not significantly changed by Dxm in LQTS1(**k**) or LQTS2 cardiomyocytes (**l**) compared to non-treated cells (*n*=10/group). (**m,n**) Current-voltage relationship of $Ba^{2+}$ recordings in Dxm-treated (*n*=10) and non-treated LQTS1 cardiomyocytes (*n*=7)(**m**) and in Dxm-treated (*n*=7) and non-treated LQTS2 cardiomyocytes (*n*=8)(**n**). (**o,p**) Representative immunoblots of human SIGMAR1, ATF4, CDK5, CDK5R1/p35 and GAPDH protein using lysates from control (Ctrl) cardiomyocytes, LQTS1 cardiomyocytes (**o**) and LQTS2 cardiomyocytes (**p**). ^, p35 antibody used for Ext. Figure 1c was discontinued (Santa Cruz, sc-820). Therefore, another antibody (Cell Signaling Technology, C64B10) was used for this blotting series while its signal-to-noise ratio was not as high as sc-820. (**q-s**) Quantification of SIGMAR1 25kDa protein band (**q, r**) and #35kDa protein band (**s**, possibly a dimer of a full-length SIGMAR1 with a SIGMAR1 splice variant[59]) in LQTS1 or LQTS2 cardiomyocytes compared to Ctrl (*n*=4/group). (**t,u**) Quantification of CDK5 (left) and CDK5R1/p35 protein expressions (right) in LQTS1 or LQTS2 cardiomyocytes compared to control cardiomyocytes (*n*=4/group). (**v,w**) Quantification of ATF4 38kDa protein band (left, non-modified), 50kDa (center, phosphorylated) and 70kDa protein expression (right, ubiquitinated) in LQTS1 or LQTS2 cardiomyocytes compared to control cardiomyocytes (*n*=4/group). All data are mean ± s.d. The treatment of Dxm or Fluvo for the experiments was 5μM, 2hrs. One-way *ANOVA* with Tukey's multiple comparisons was used for a,b,c,d,e,f. Unpaired two-tailed Student's *t*-test was used for k,l,q,r,s,t,u,v,w between the groups and for g,h,m,n at each voltage step. * $P<0.05$, ** $P<0.01$, n.s., not significant. The cardiomyocytes were from at least two independent differentiations.

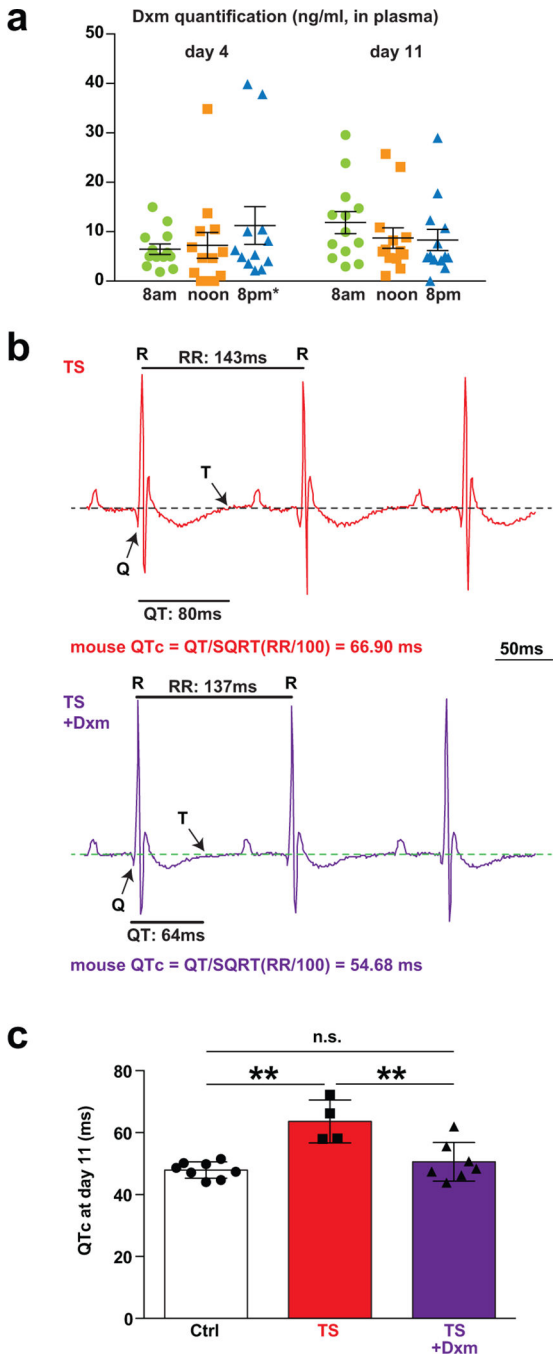


**Extended Data Figure 8 |. The effect of dextromethorphan on Timothy syndrome mouse model.** (**a**) Plasma dextromethorphan (Dxm) concentrations in control mice at day 4 and day 11 after continuous dosing of Dxm in drinking water ($n$=13, mean ± s.e.m.). Dxm was provided in water since day 1 at 8am. * 8 p.m. time point at day 4 had an outlier defined by statistics and the outlier was excluded from the final analysis. (**b**) Representative analysis procedures for ECG traces in Timothy syndrome (TS) mice without treatment or treated with Dxm at day 4 (also used in Figure 5c,d). (**c**) QT intervals were significantly shortened by Dxm treatment in TS mice at day 11 ($n$=8 for ctrl, $n$=4 for TS, $n$=7 for TS+Dxm, female, 12-week

old). Three mouse heart samples from each group were used for the global proteomics analysis. All data of Ext. Figure 8 are mean ± s.d. except Ext. Figure 8a. One-way *ANOVA* with Tukey's multiple comparisons were used for statistics. ** $P$<0.01, n.s., not significant.

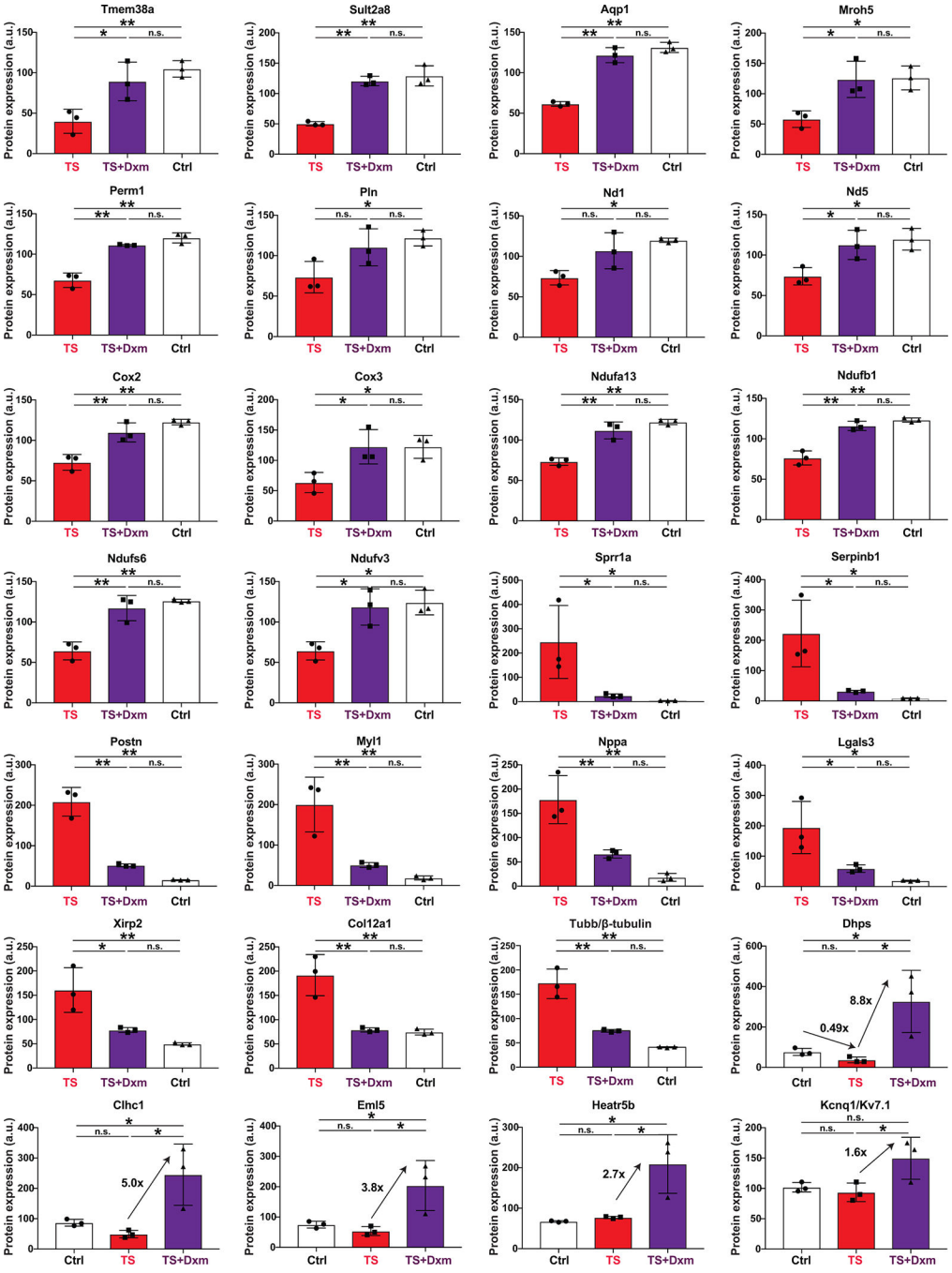


**Extended Data Figure 9 |. The effect of dextromethorphan on the protein expression in mouse hearts.**

Altered protein expressions between control hearts (Ctrl), non-treated (TS) and Dxm-treated TS hearts (TS+Dxm) ($n$=3/group). A comprehensive heat map and summary of proteomics

results are shown in Figure 5e. All data are mean ± s.d. One-way *ANOVA* with Tukey's multiple comparisons was used. * $P<0.05$, ** $P<0.01$, n.s., not significant.

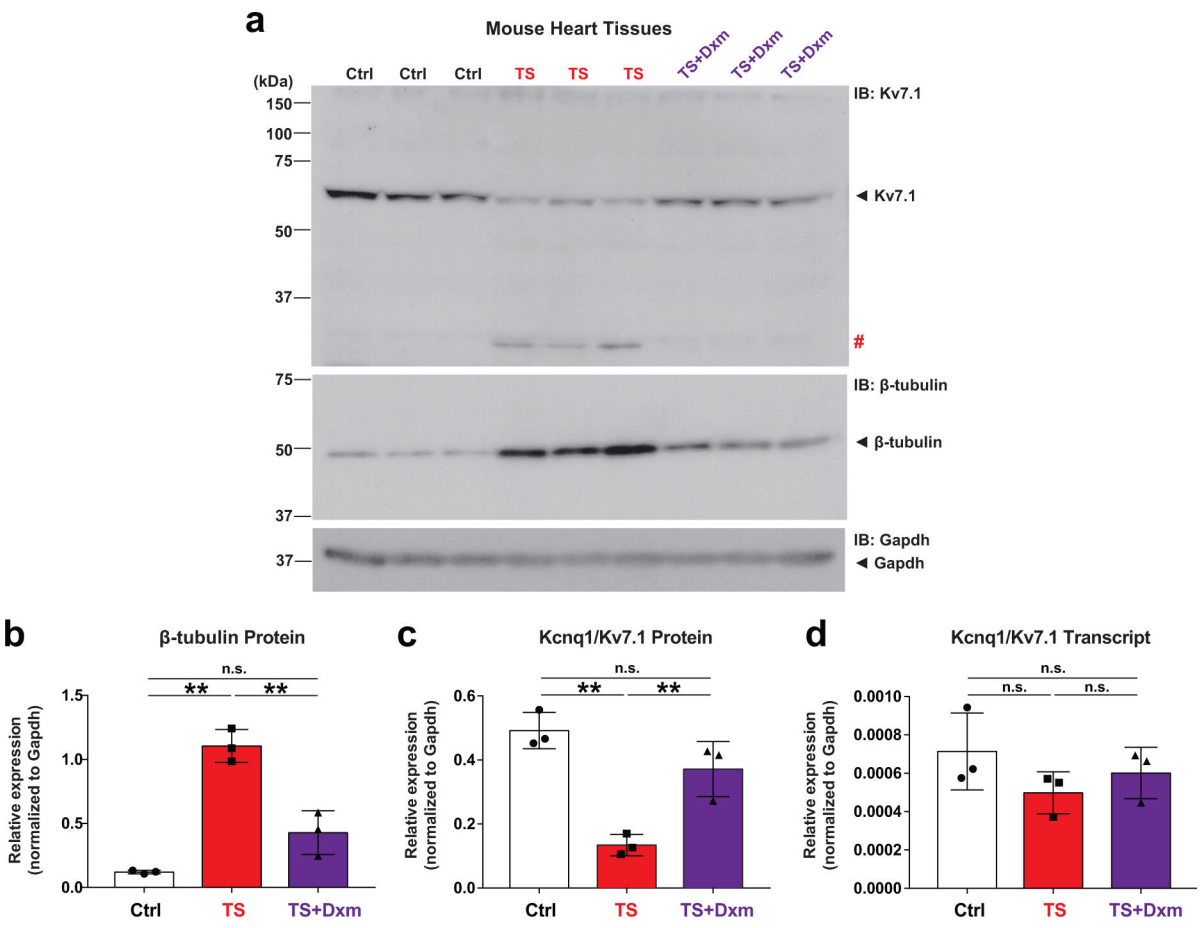


**Extended Data Figure 10 |. The effect of dextromethorphan on $K_V$7.1 protein expression in mouse hearts.**

(**a**) Representative immunoblots of $K_V$7.1, β-tubulin and Gapdh protein using mouse heart lysates from TS (non-treated and Dxm-treated) mice and the control littermates (Ctrl) at day 11 (each, $n$=3, using the same samples with the global proteomics shown in Figure 5e). #, bands indicate putative degradation of $K_V$7.1 in TS mouse hearts. (**b-c**) Quantification of β-tubulin (**b**) and Kcnq1/$K_V$7.1 protein expression (**c**, normalized to Gapdh) in TS (non-treated and Dxm-treated) and Ctrl mouse hearts ($n$=3/group). Altered β-tubulin expression has been reported previously in animal model of myocardial infarction and Gapdh was recommended as a more reliable loading control for Western blot analyses[60]. (**d**) *Kcnq1/* $K_V$7.1 mRNA expression (normalized to Gapdh) in TS (non-treated and Dxm-treated) and Ctrl mouse hearts ($n$=3/group). All data are mean ± s.d. One-way *ANOVA* with Tukey's multiple comparisons was used. ** $P<0.01$, n.s., not significant.

## Supplementary Material

Refer to Web version on PubMed Central for supplementary material.

## Acknowledgements

We thank J.C. Wu (Stanford University) for sharing long QT type 1 and 2 iPSC lines; G. Pitt (Weill Cornell Medicine), R. Katz, A. Rinderspacher, S. Deng, B. Corneo, R. Robinson, H. Colecraft, S. Marx, R. Kass, E. Passague and J. Stein (Columbia University) and R. Kaye (SSI Strategy) for helpful discussions; S. Asano (Pfizer Inc.) for helpful inputs on image analysis. This work was supported by NIH K99/R00HL111345, NIH R01HL138486, Columbia University Core Usage Funding Program and Helmsley Stem Cell Seed Grant (to M.Y.), NIH R01 HL136758 (to J.P.M), NIH F31HL142239 (to J.R.Q.), JSPS postdoc fellowship (to K.M.) and Columbia TRANSFROM TL1 training program (to R.B. and D.A.).

## Reference:

1. Berridge MJ, Bootman MD & Roderick HL Calcium signalling: dynamics, homeostasis and remodelling. Nat Rev Mol Cell Biol 4, 517–529, doi:10.1038/nrm1155nrm1155 [pii] (2003). [PubMed: 12838335]
2. Wagner S, Maier LS & Bers DM Role of sodium and calcium dysregulation in tachyarrhythmias in sudden cardiac death. Circ Res 116, 1956–1970, doi:10.1161/CIRCRESAHA.116.304678 (2015). [PubMed: 26044250]
3. Splawski I et al. Ca(V)1.2 calcium channel dysfunction causes a multisystem disorder including arrhythmia and autism. Cell 119, 19–31, doi:10.1016/j.cell.2004.09.011S0092867404008426 [pii] (2004). [PubMed: 15454078]
4. Mahida S et al. Genetics of congenital and drug-induced long QT syndromes: current evidence and future research perspectives. J Interv Card Electrophysiol 37, 9–19, doi:10.1007/s10840-013-9779-5 (2013). [PubMed: 23515882]
5. Yazawa M et al. Using induced pluripotent stem cells to investigate cardiac phenotypes in Timothy syndrome. Nature 471, 230–234, doi:10.1038/nature09855 (2011). [PubMed: 21307850]
6. Song L, Park SE, Isseroff Y, Morikawa K & Yazawa M Inhibition of CDK5 Alleviates the Cardiac Phenotypes in Timothy Syndrome. Stem Cell Reports 9, 50–57, doi:10.1016/j.stemcr.2017.05.028 (2017). [PubMed: 28648896]
7. Massard C et al. A first in man, phase I dose-escalation study of PHA-793887, an inhibitor of multiple cyclin-dependent kinases (CDK2, 1 and 4) reveals unexpected hepatotoxicity in patients with solid tumors. Cell Cycle 10, 963–970, doi:10.4161/cc.10.6.15075 (2011). [PubMed: 21368575]
8. Malumbres M Cyclin-dependent kinases. Genome biology 15, 122, doi:10.1186/gb4184 (2014). [PubMed: 25180339]
9. Maurice T & Goguadze N Sigma-1 (sigma1) Receptor in Memory and Neurodegenerative Diseases. Handb Exp Pharmacol 244, 81–108, doi:10.1007/164_2017_15 (2017). [PubMed: 28275911]
10. Kim FJ & Maher CM Sigma1 Pharmacology in the Context of Cancer. Handbook of experimental pharmacology 244, 237–308, doi:10.1007/164_2017_38 (2017). [PubMed: 28744586]
11. Ruscher K & Wieloch T The involvement of the sigma-1 receptor in neurodegeneration and neurorestoration. J Pharmacol Sci 127, 30–35, doi:10.1016/j.jphs.2014.11.011 (2015). [PubMed: 25704015]
12. Morales-Lazaro SL, Gonzalez-Ramirez R & Rosenbaum T Molecular Interplay Between the Sigma-1 Receptor, Steroids, and Ion Channels. Front Pharmacol 10, 419, doi:10.3389/fphar.2019.00419 (2019). [PubMed: 31068816]
13. Tsai SY, Pokrass MJ, Klauer NR, Nohara H & Su TP Sigma-1 receptor regulates Tau phosphorylation and axon extension by shaping p35 turnover via myristic acid. Proc Natl Acad Sci U S A 112, 6742–6747, doi:10.1073/pnas.1422001112 (2015). [PubMed: 25964330]
14. Schmidt HR et al. Crystal structure of the human sigma1 receptor. Nature 532, 527–530, doi:10.1038/nature17391 (2016). [PubMed: 27042935]
15. Su TP et al. Sigma compounds derived from phencyclidine: identification of PRE-084, a new, selective sigma ligand. J Pharmacol Exp Ther 259, 543–550 (1991). [PubMed: 1658302]
16. Figgitt DP & McClellan KJ Fluvoxamine. An updated review of its use in the management of adults with anxiety disorders. Drugs 60, 925–954 (2000). [PubMed: 11085201]

17. Nguyen L, Robson MJ, Healy JR, Scandinaro AL & Matsumoto RR Involvement of sigma-1 receptors in the antidepressant-like effects of dextromethorphan. PLoS One 9, e89985, doi:10.1371/journal.pone.0089985 (2014). [PubMed: 24587167]
18. De Blasio F et al. Cough management: a practical approach. Cough 7, 7, doi:10.1186/1745-9974-7-7 (2011). [PubMed: 21985340]
19. Taylor CP, Traynelis SF, Siffert J, Pope LE & Matsumoto RR Pharmacology of dextromethorphan: Relevance to dextromethorphan/quinidine (Nuedexta(R)) clinical use. Pharmacol Ther 164, 170–182, doi:10.1016/j.pharmthera.2016.04.010 (2016). [PubMed: 27139517]
20. Rosen H Dextromethorphan/quinidine sulfate for pseudobulbar affect. Drugs Today (Barc) 44, 661–668, doi:10.1358/dot.2008.44.9.1258664 (2008). [PubMed: 19137121]
21. Chaki S, Tanaka M, Muramatsu M & Otomo S NE-100, a novel potent sigma ligand, preferentially binds to sigma 1 binding sites in guinea pig brain. Eur J Pharmacol 251, R1–2, doi:10.1016/0014-2999(94)90453-7 (1994). [PubMed: 8137864]
22. Okuyama S et al. NE-100, a novel sigma receptor ligand: in vivo tests. Life Sci 53, PL285–290, doi:10.1016/0024-3205(93)90588-t (1993). [PubMed: 7901723]
23. Tanaka M, Shirasaki T, Kaku S, Muramatsu M & Otomo S Characteristics of binding of [3H]NE-100, a novel sigma-receptor ligand, to guinea-pig brain membranes. Naunyn Schmiedebergs Arch Pharmacol 351, 244–251, doi:10.1007/BF00233243 (1995). [PubMed: 7609777]
24. Mitsuda T et al. Sigma-1Rs are upregulated via PERK/eIF2alpha/ATF4 pathway and execute protective function in ER stress. Biochem Biophys Res Commun 415, 519–525, doi:10.1016/j.bbrc.2011.10.113 (2011). [PubMed: 22079628]
25. Bhuiyan MS, Tagashira H & Fukunaga K Sigma-1 receptor stimulation with fluvoxamine activates Akt-eNOS signaling in the thoracic aorta of ovariectomized rats with abdominal aortic banding. Eur J Pharmacol 650, 621–628, doi:10.1016/j.ejphar.2010.10.055 (2011). [PubMed: 21044620]
26. Montastruc G et al. Drugs and dilated cardiomyopathies: A case/noncase study in the French PharmacoVigilance Database. Br J Clin Pharmacol 69, 287–294, doi:10.1111/j.1365-2125.2009.03596.x (2010). [PubMed: 20233200]
27. Hashimoto K Sigma-1 receptors and selective serotonin reuptake inhibitors: clinical implications of their relationship. Cent Nerv Syst Agents Med Chem 9, 197–204 (2009). [PubMed: 20021354]
28. Chen TW et al. Ultrasensitive fluorescent proteins for imaging neuronal activity. Nature 499, 295–300, doi:10.1038/nature12354 (2013). [PubMed: 23868258]
29. Mueller BH 2nd et al. Sigma-1 receptor stimulation attenuates calcium influx through activated L-type Voltage Gated Calcium Channels in purified retinal ganglion cells. Exp Eye Res 107, 21–31, doi:10.1016/j.exer.2012.11.002 (2013). [PubMed: 23183135]
30. Pan B, Guo Y, Kwok WM, Hogan Q & Wu HE Sigma-1 receptor antagonism restores injury-induced decrease of voltage-gated Ca2+ current in sensory neurons. J Pharmacol Exp Ther 350, 290–300, doi:10.1124/jpet.114.214320 (2014). [PubMed: 24891452]
31. Tchedre KT et al. Sigma-1 receptor regulation of voltage-gated calcium channels involves a direct interaction. Invest Ophthalmol Vis Sci 49, 4993–5002, doi:10.1167/iovs.08-1867 (2008). [PubMed: 18641291]
32. Crottes D et al. Sig1R protein regulates hERG channel expression through a post-translational mechanism in leukemic cells. J Biol Chem 286, 27947–27958, doi:10.1074/jbc.M111.226738 (2011). [PubMed: 21680736]
33. Balasuriya D et al. A direct interaction between the sigma-1 receptor and the hERG voltage-gated K+ channel revealed by atomic force microscopy and homogeneous time-resolved fluorescence (HTRF(R)). J Biol Chem 289, 32353–32363, doi:10.1074/jbc.M114.603506 (2014). [PubMed: 25266722]
34. Wu ZY, Yu DJ, Soong TW, Dawe GS & Bian JS Progesterone impairs human ether-a-go-go-related gene (HERG) trafficking by disruption of intracellular cholesterol homeostasis. J Biol Chem 286, 22186–22194, doi:10.1074/jbc.M110.198853 (2011). [PubMed: 21525004]
35. Liang P et al. Drug screening using a library of human induced pluripotent stem cell-derived cardiomyocytes reveals disease-specific patterns of cardiotoxicity. Circulation 127, 1677–1691, doi:10.1161/CIRCULATIONAHA.113.001883 (2013). [PubMed: 23519760]

36. Mehta A et al. Re-trafficking of hERG reverses long QT syndrome 2 phenotype in human iPS-derived cardiomyocytes. Cardiovasc Res 102, 497–506, doi:10.1093/cvr/cvu060 (2014). [PubMed: 24623279]
37. Pasca SP et al. Using iPSC-derived neurons to uncover cellular phenotypes associated with Timothy syndrome. Nat Med 17, 1657–1662, doi:10.1038/nm.2576 (2011). [PubMed: 22120178]
38. Salama G & London B Mouse models of long QT syndrome. J Physiol 578, 43–53, doi:10.1113/jphysiol.2006.118745 (2007). [PubMed: 17038432]
39. Landry NM, Cohen S & Dixon IMC Periostin in cardiovascular disease and development: a tale of two distinct roles. Basic Res Cardiol 113, 1, doi:10.1007/s00395-017-0659-5 (2018). [PubMed: 29101484]
40. McCalmon SA et al. Modulation of angiotensin II-mediated cardiac remodeling by the MEF2A target gene Xirp2. Circ Res 106, 952–960, doi:10.1161/CIRCRESAHA.109.209007 (2010). [PubMed: 20093629]
41. Yazawa M et al. TRIC channels are essential for Ca2+ handling in intracellular stores. Nature 448, 78–82, doi:10.1038/nature05928 (2007). [PubMed: 17611541]
42. Brandt RR, Wright RS, Redfield MM & Burnett JC Jr. Atrial natriuretic peptide in heart failure. J Am Coll Cardiol 22, 86A–92A, doi:10.1016/0735-1097(93)90468-g (1993).
43. Thiel WH et al. Proarrhythmic defects in Timothy syndrome require calmodulin kinase II. Circulation 118, 2225–2234, doi:CIRCULATIONAHA.108.788067 [pii] 10.1161/CIRCULATIONAHA.108.788067 (2008). [PubMed: 19001023]
44. Ottolia M, Torres N, Bridge JH, Philipson KD & Goldhaber JI Na/Ca exchange and contraction of the heart. J Mol Cell Cardiol 61, 28–33, doi:10.1016/j.yjmcc.2013.06.001 (2013). [PubMed: 23770352]
45. Deisemann H et al. Effects of common antitussive drugs on the hERG potassium channel current. J Cardiovasc Pharmacol 52, 494–499, doi:10.1097/FJC.0b013e31818eec8d (2008). [PubMed: 19034038]
46. Itzhaki I et al. Modelling the long QT syndrome with induced pluripotent stem cells. Nature 471, 225–229, doi:10.1038/nature09747 (2011). [PubMed: 21240260]
47. Uresin Y, Ozek M & Sevgi S Protective effects of dextromethorphan and tizanidine on ouabain-induced arrhythmias. Methods Find Exp Clin Pharmacol 24, 421–423, doi:10.1358/mf.2002.24.7.696543 (2002). [PubMed: 12428430]
48. Boland DM, Rein J, Lew EO & Hearn WL Fatal cold medication intoxication in an infant. J Anal Toxicol 27, 523–526, doi:10.1093/jat/27.7.523 (2003). [PubMed: 14607011]
49. Kaplan B, Buchanan J & Krantz MJ QTc prolongation due to dextromethorphan. Int J Cardiol 148, 363–364, doi:10.1016/j.ijcard.2010.09.024 (2011). [PubMed: 20947192]
50. Nitert MD, Nagorny CL, Wendt A, Eliasson L & Mulder H CaV1.2 rather than CaV1.3 is coupled to glucose-stimulated insulin secretion in INS-1 832/13 cells. J Mol Endocrinol 41, 1–11, doi:10.1677/JME-07-0133 (2008). [PubMed: 18562674]
51. Stracina T & Novakova M Cardiac sigma receptors - an update. Physiol Res 67, S561–S576, doi:10.33549/physiolres.934052 (2018). [PubMed: 30607964]
52. Lewis R, Li J, McCormick PJ, C LHH & Jeevaratnam K Is the sigma-1 receptor a potential pharmacological target for cardiac pathologies? A systematic review. Int J Cardiol Heart Vasc 26, 100449, doi:10.1016/j.ijcha.2019.100449 (2020). [PubMed: 31909177]
53. Reis G et al. Effect of early treatment with fluvoxamine on risk of emergency care and hospitalisation among patients with COVID-19: the TOGETHER randomised, platform clinical trial. Lancet Glob Health, doi:10.1016/S2214-109X(21)00448-4 (2021).
54. Gordon DE et al. A SARS-CoV-2 protein interaction map reveals targets for drug repurposing. Nature 583, 459–468, doi:10.1038/s41586-020-2286-9 (2020). [PubMed: 32353859]
55. Song L et al. Dual optical recordings for action potentials and calcium handling in induced pluripotent stem cell models of cardiac arrhythmias using genetically encoded fluorescent indicators. Stem Cells Transl Med 4, 468–475, doi:10.5966/sctm.2014-0245 (2015). [PubMed: 25769651]
56. Skarnes WC, Pellegrino E & McDonough JA Improving homology-directed repair efficiency in human stem cells. Methods 164–165, 18–28, doi:10.1016/j.ymeth.2019.06.016 (2019).

57. Navarrete-Perea J, Yu Q, Gygi SP & Paulo JA Streamlined Tandem Mass Tag (SL-TMT) Protocol: An Efficient Strategy for Quantitative (Phospho)proteome Profiling Using Tandem Mass Tag-Synchronous Precursor Selection-MS3. J Proteome Res 17, 2226–2236, doi:10.1021/acs.jproteome.8b00217 (2018). [PubMed: 29734811]

58. Tyanova S et al. The Perseus computational platform for comprehensive analysis of (prote)omics data. Nat Methods 13, 731–740, doi:10.1038/nmeth.3901 (2016). [PubMed: 27348712]

59. Pan L et al. Isolation and characterization of alternatively spliced variants of the mouse sigma1 receptor gene, Sigmar1. PLoS One 12, e0174694, doi:10.1371/journal.pone.0174694 (2017). [PubMed: 28350844]

60. Nie X et al. An appropriate loading control for western blot analysis in animal models of myocardial ischemic infarction. Biochem Biophys Rep 12, 108–113, doi:10.1016/j.bbrep.2017.09.001 (2017). [PubMed: 28955798]

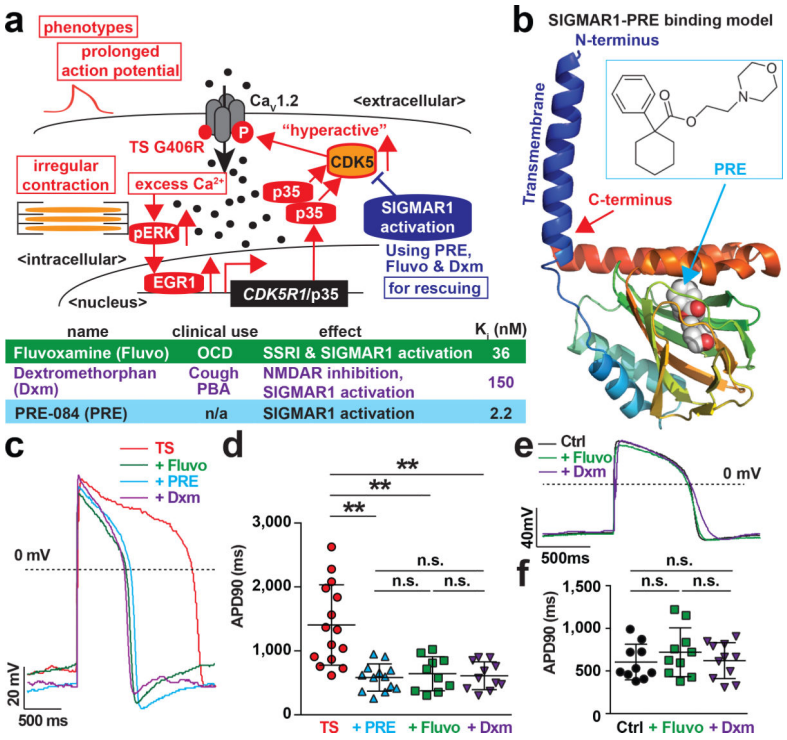


**Figure 1 |. The effect of SIGMAR1 agonists on the phenotypes in cardiac action potentials in Timothy syndrome iPSC-derived cardiomyocytes.**

(**a**) Schematic representation of altered molecules (red)[6] and therapeutic strategy using SIGMAR1 agonists (blue) in Timothy syndrome (TS) cardiomyocytes. The bottom table shows the characteristics of SIGMAR1 agonists. OCD, obsessive compulsive disorder. PBA, Pseudo Bulbar Affect. SSRI, selective serotonin reuptake inhibitor. NMDAR, *N*-Methyl-D-aspartate receptor. (**b**) Docking model of SIGMAR1 and its agonist PRE-084. (**c**) Representative traces of 0.2Hz-paced action potentials in TS cardiomyocytes without treatment or treated with SIGMAR1 agonists, PRE-084 (+PRE), fluvoxamine (+Fluvo) or dextromethorphan (+Dxm). (**d**) Action potential duration (APD90, 90% reduction from peak) analysis in TS cardiomyocytes without treatment ($n$=15) or treated with PRE ($n$=13), Fluvo ($n$=10) and Dxm ($n$=11). Other action potential parameters are shown in Ext. Figure 2a–c. (**e**) Representative traces of 0.5Hz-paced action potentials in isogenic control (Ctrl) iPSC-derived cardiomyocytes without treatment or treated with Dxm or Fluvo. (**f**) APD90 analysis in the control cells without treatment ($n$=10) or treated with Dxm ($n$=11) or Fluvo ($n$=10). Other action potential parameters of isogenic Ctrl are shown in Ext. Figure 2d–f. All data are mean ± s.d. The treatment of PRE, Fluvo and Dxm for the experiments was 5μM, 2hrs. One-way *ANOVA* with Tukey's multiple comparisons was used for d, f. $^{**}P<0.01$, n.s., not significant. The cardiomyocytes were from at least two independent differentiations.

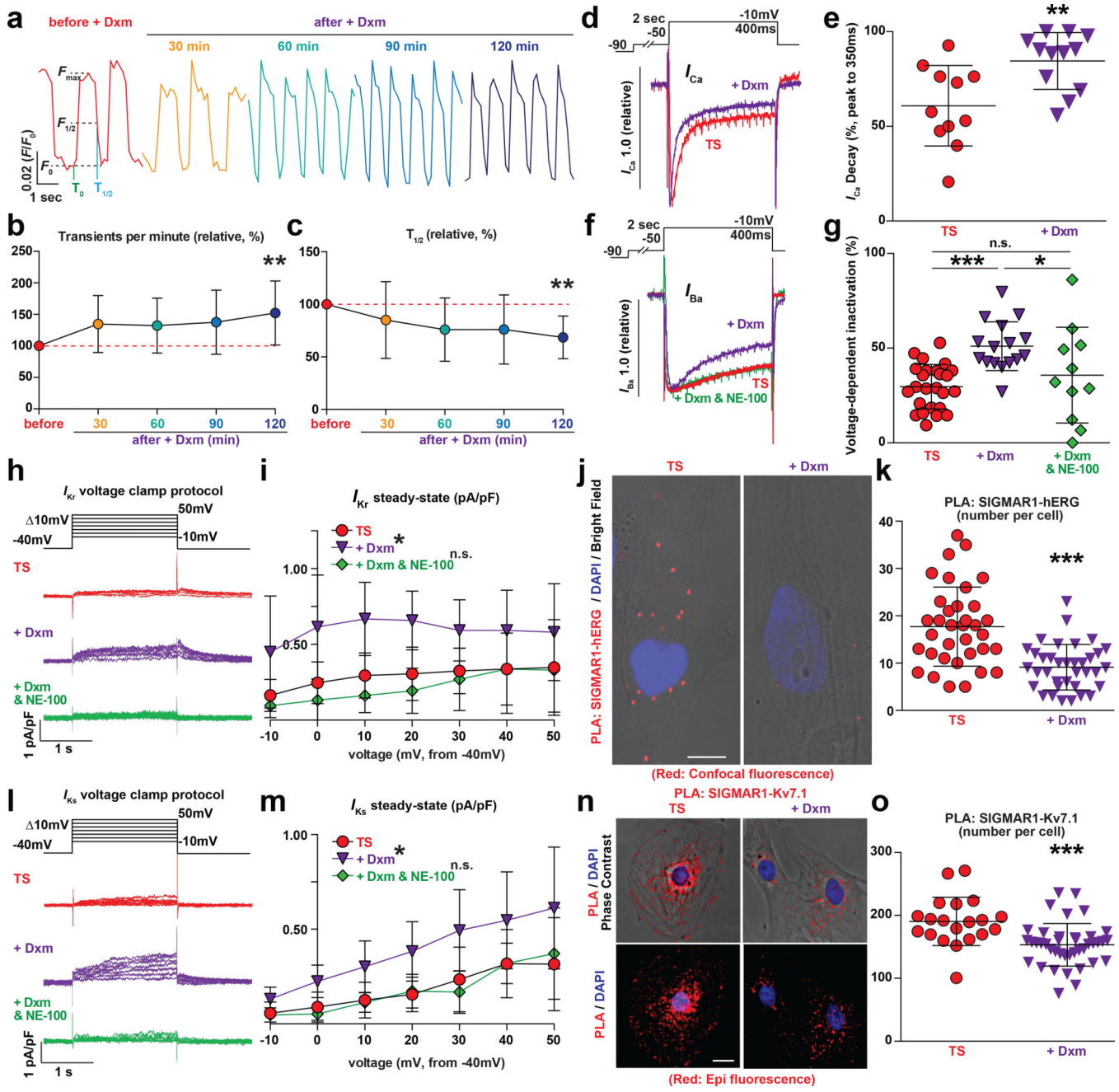


**Figure 2 |. The effect of dextromethorphan on cardiac calcium handling and ion channels in human iPSC model of Timothy syndrome.**

(**a**) Representative traces of time-course calcium imaging in spontaneously contracting Timothy syndrome (TS) cardiomyocytes treated with Dxm (5μM, until 120min). (**b-c**) Calcium transient frequency (**b**) and duration(**c**) analysis in TS cardiomyocytes before and after Dxm treatment ($n$=19). (**d**) Representative traces of $Ca^{2+}$ currents in TS cardiomyocytes with and without Dxm. (**e**) Late calcium current analysis in TS cardiomyocytes with and without Dxm (TS, $n$=11; +Dxm, $n$=12). (**f**) Representative traces of $Ba^{2+}$ currents in TS cardiomyocytes without treatment, with Dxm (5μM, 2hrs,

+Dxm) or Dxm with a SIGMAR1 antagonist, NE-100 (1μM, +Dxm&NE-100). (**g**) Voltage-dependent inactivation in TS cardiomyocytes without treatment ($n$=25), with Dxm ($n$=16) or Dxm+NE-100 ($n$=11). (**h**) Representative traces of $I_{Kr}$ currents (E-4031-sensitive) in TS cardiomyocytes with Dxm (5μM), Dxm&NE-100 (each, 5μM) or without treatment. (**i**) $I_{Kr}$ current amplitude analysis in TS cardiomyocytes with Dxm ($n$=9), Dxm&NE-100 ($n$=10) or without treatment ($n$=10) (* $P$<0.05, Dxm vs TS and Dxm vs Dxm & NE-100, at −10, 0, 10, 20 and 30mV). (**j**) Representative confocal fluorescent and bright-field images of TS cardiomyocytes without and with Dxm treatment (+Dxm) from proximity ligation assay (PLA, SIGMAR1-hERG, red, DAPI, blue). Scale bar, 10μm. (**k**) SIGMAR1-hERG PLA quantification in Dxm-treated ($n$=36) and non-treated ($n$=35) TS cardiomyocytes. (**l**) Representative traces of $I_{Ks}$ currents (Chromanol-293B-sensitive) in TS cardiomyocytes treated with Dxm (5μM), Dxm&NE-100 (each, 5μM) or without treatment. (**m**) $I_{Ks}$ current amplitude analysis in TS cardiomyocytes with Dxm ($n$=10), Dxm&NE-100 ($n$=9) or without treatment ($n$=10) (* $P$<0.05, Dxm vs TS and Dxm vs Dxm & NE-100, at −10, 0, 10, 20, 30 and 40mV). (**n**) Representative epi-fluorescent and phase-contrast images of TS cardiomyocytes without and with Dxm treatment (+Dxm) from PLA (SIGMAR1-$K_V$7.1, red, DAPI, blue). Scale bar, 10μm. (**o**) SIGMAR1-$K_V$7.1 PLA quantification in Dxm-treated ($n$=40) and non-treated ($n$=20) TS cardiomyocytes. All data are mean ± s.d. One-way *ANOVA* with Tukey's multiple comparisons was used for b, c, g between the groups and for i, m at each voltage step. Unpaired two-tailed Student's $t$-test was used for e, k, o. * $P$<0.05, ** $P$<0.01, *** $P$<0.001, n.s., not significant. The samples were from at least two independent differentiations.

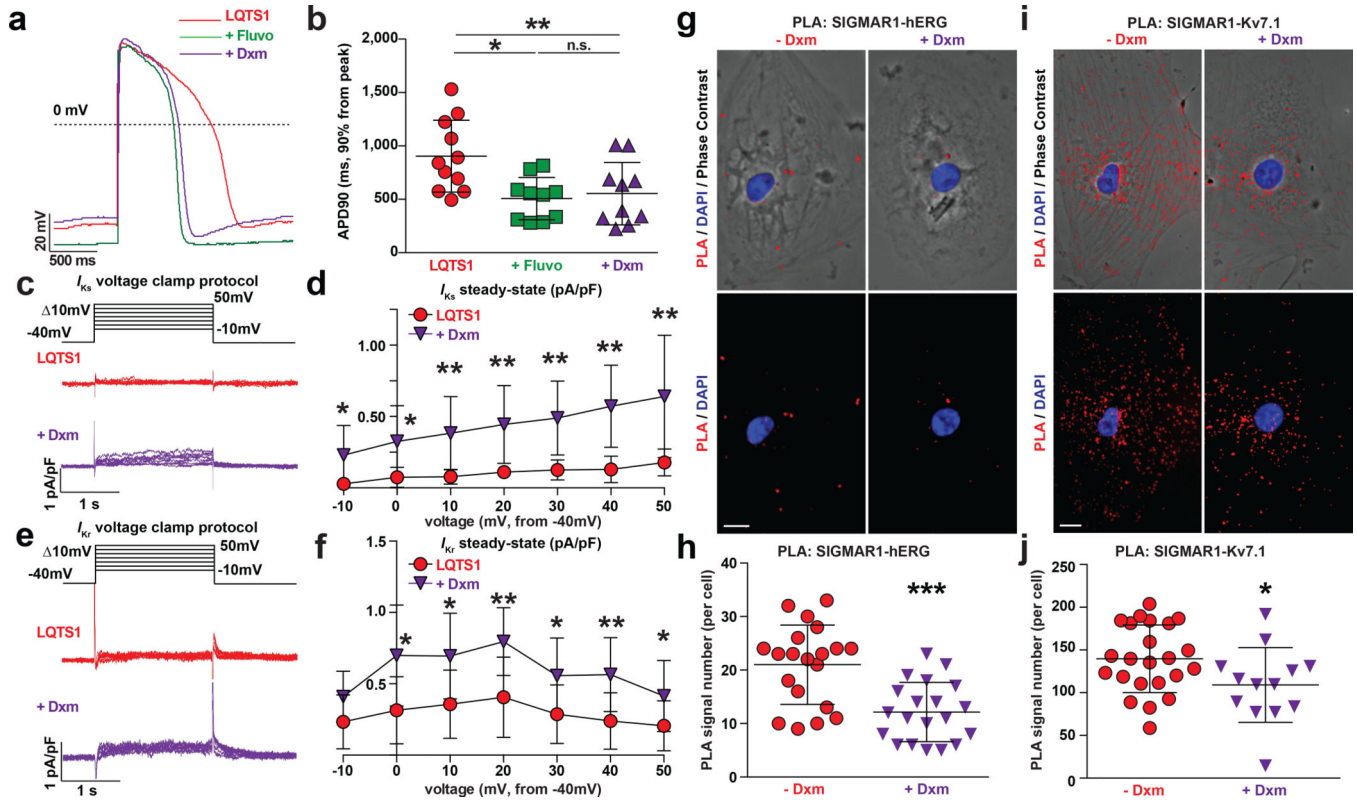


**Figure 3 |. The effect of dextromethorphan on the phenotypes in long QT syndrome type 1.**

(**a**) Representative traces of action potentials in long QT syndrome type 1 (LQTS1) iPSC-derived cardiomyocytes without treatment or treated with fluvoxamine (+Fluvo) or dextromethorphan (+Dxm). (**b**) Action potential duration (APD90) analysis in LQTS1 cardiomyocytes without treatment ($n$=11) or treated with fluvoxamine ($n$=10) or dextromethorphan ($n$=10). Other action potential parameters are shown in Ext. Figure 7a, c, e. (**c**) Representative traces of $I_{Ks}$ currents (Chromanol-293B-sensitive) in LQTS1 cardiomyocytes treated with Dxm or without treatment. (**d**) $I_{Ks}$ currents (steady-state) were significantly increased by Dxm in LQTS1 cardiomyocytes at all voltage steps ($n$=10/group). (**e**) Representative traces of $I_{Kr}$ currents (E-4031-sensitive) in LQTS1 cardiomyocytes treated with Dxm or without treatment. (**f**) $I_{Kr}$ currents (steady-state) were significantly increased in Dxm-treated LQTS1 cardiomyocytes ($n$=9) at 0, 10, 20, 30, 40 and 50mV steps compared with LQTS1 cardiomyocytes without treatment ($n$=10). (**g**) Representative epi-fluorescent and phase-contrast images of LQTS1 cardiomyocytes with and without Dxm treatment from proximity ligation assay (PLA, SIGMAR1-hERG, red, DAPI, blue). Scale bar, 10μm. (**h**) SIGMAR1-hERG PLA quantification in Dxm-treated ($n$=20) and non-treated ($n$=20) LQTS1 cardiomyocytes. (**i**) Representative epi-fluorescent and phase-contrast images of LQTS1 cardiomyocytes with and without Dxm treatment from PLA (SIGMAR1-$K_V$7.1, red, DAPI, blue). Scale bar, 10μm. (**j**) SIGMAR1-$K_V$7.1 PLA quantification in Dxm-treated ($n$=13) and non-treated ($n$=23) LQTS1 cardiomyocytes. All data are mean ± s.d. The treatment of Fluvo or Dxm for the experiments was 5μM, 2hrs. One-way *ANOVA* with Tukey's multiple comparisons was used for b, and unpaired two-tailed Student's $t$-test was used for h, j between the groups and for d, f at each voltage step. * $P$<0.05, ** $P$<0.01,

*** $P<0.001$, n.s., not significant. The cardiomyocytes were from at least two independent differentiations.

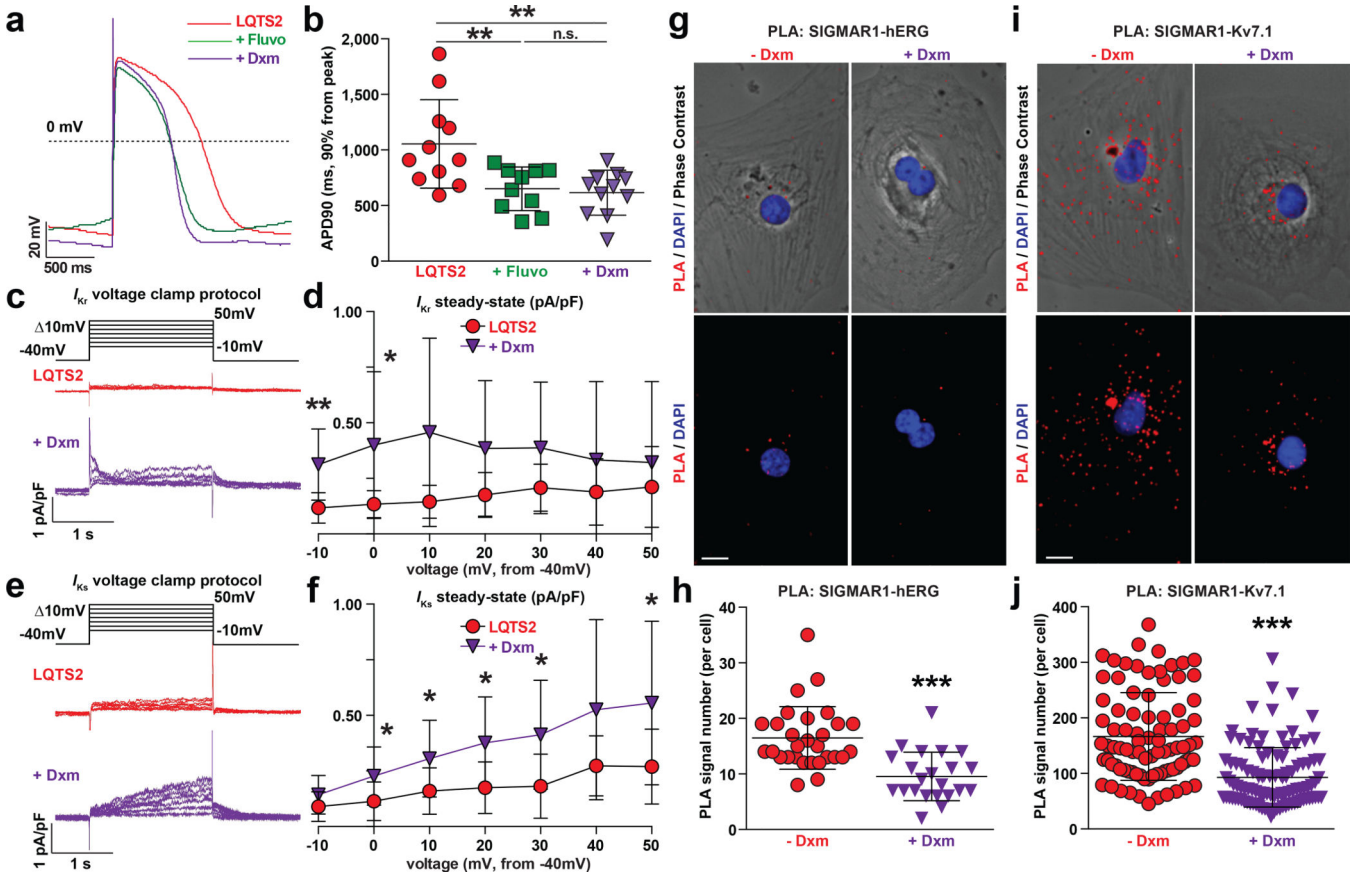


**Figure 4 |. The effect of dextromethorphan on the phenotypes in long QT syndrome type 2.**

(**a**) Representative traces of action potentials in long QT syndrome type 2 (LQTS2) iPSC-derived cardiomyocytes without treatment or treated with fluvoxamine (+Fluvo) or dextromethorphan (+Dxm). (**b**) Action potential duration (APD90) analysis in LQTS2 cardiomyocytes without treatment ($n$=11) or treated with fluvoxamine ($n$=10) or dextromethorphan ($n$=11). Other action potential parameters are shown in Ext. Figure 7b, d, f. (**c**) Representative traces of $I_{Kr}$ currents (E-4031-sensitive) in LQTS2 cardiomyocytes treated with Dxm or without treatment. (**d**) $I_{Kr}$ currents (steady-state) were significantly increased in Dxm-treated LQTS2 cardiomyocytes ($n$=9) at −10 and 0mV steps compared with LQTS2 cardiomyocytes without treatment ($n$=10). (**e**) Representative traces of $I_{Ks}$ currents (Chromanol-293B-sensitive) in LQTS2 cardiomyocytes treated with Dxm or without treatment. (**f**) $I_{Ks}$ currents (steady-state) were significantly increased in Dxm-treated LQTS2 cardiomyocytes at 0, 10, 20, 30 and 50mV steps compared with LQTS2 cardiomyocytes without treatment ($n$=10/group). (**g**) Representative epi-fluorescent and phase-contrast images of LQTS2 cardiomyocytes with and without Dxm treatment from proximity ligation assay (PLA, SIGMAR1-hERG, red, DAPI, blue). Scale bar, 10μm. (**h**) SIGMAR1-hERG PLA quantification in Dxm-treated ($n$=22) and non-treated ($n$=29) LQTS2 cardiomyocytes. (**i**) Representative epi-fluorescent and phase-contrast images of LQTS2 cardiomyocytes with and without Dxm treatment from PLA (SIGMAR1-$K_V$7.1, red, DAPI, blue). Scale bar, 10μm. (**j**) SIGMAR1-$K_V$7.1 PLA quantification in Dxm-treated ($n$=107) and non-treated ($n$=87) LQTS2 cardiomyocytes. All data are mean ± s.d. The treatment of

Fluvo or Dxm for the experiments was 5μM, 2hrs. One-way *ANOVA* with Tukey's multiple comparisons was used for b. Unpaired two-tailed Student's *t*-test was used for h, j between the groups and for d, f at each voltage step. * $P<0.05$, ** $P<0.01$, *** $P<0.001$, n.s., not significant. The cardiomyocytes were from at least two independent differentiations.

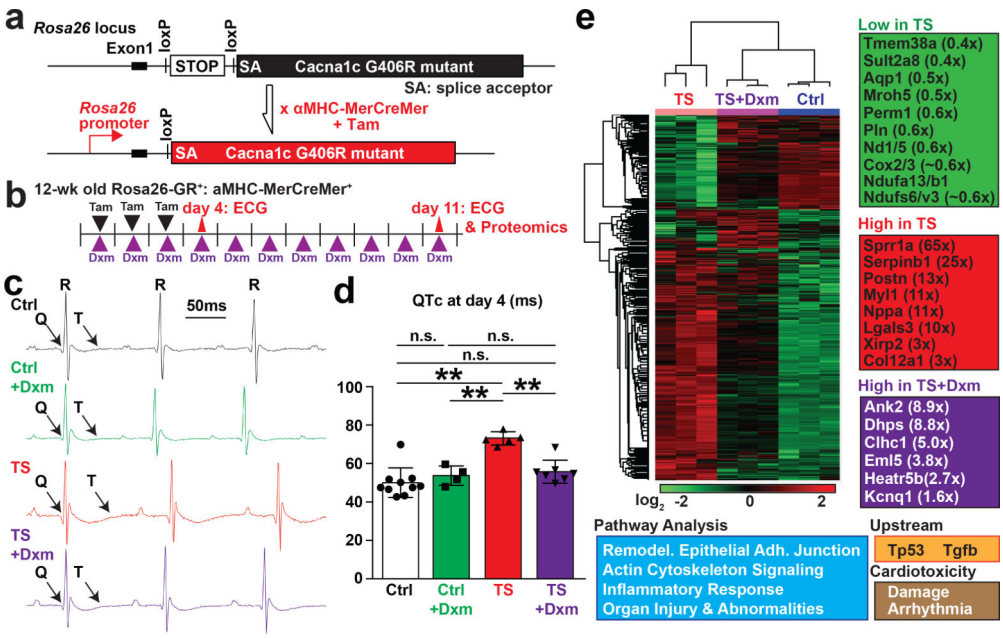


**Figure 5 |. The effect of dextromethorphan on Timothy syndrome mouse model.**

(**a**) Targeting design of Timothy syndrome mutant (G406R in the calcium channel *Cacna1c* gene) in mouse *Rosa26* locus and the breeding strategy for inducing cardiac specific tamoxifen (Tam) inducible expression of Timothy syndrome mutant channels. (**b**) Experimental design for the induction of Timothy syndrome mutant channel expression in heart with Tam and the *in vivo* testing of dextromethorphan (Dxm). Dxm was dosed in drinking water and the pharmacokinetic analysis of plasma Dxm concentrations at day 4 and day 11 are shown in Ext. Figure 8a. (**c**) Representative traces of electrocardiography (ECG) in Timothy syndrome mice (TS) and the control littermates (Ctrl) without treatment or treated with Dxm (+Dxm) at day 4. (**d**) Prolonged QT intervals in Timothy syndrome mice were normalized by Dxm ($n$=10 for Ctrl, $n$=4 for Ctrl+Dxm, $n$=5 for TS, $n$=7 for TS+Dxm). QT intervals were corrected using mouse formula (QTc, Ext. Figure 8b). One-way *ANOVA* with Sidak's multiple comparisons was used (** $P$<0.01; n.s., not significant). (**e**) Proteomics analysis including heat map comparisons and pathway analysis at day 11 in control hearts, non-treated and Dxm-treated Timothy syndrome hearts ($n$=3/group). ECG at day 11 also confirmed the beneficial effect of Dxm on QT prolongation in the mutant mice (Ext. Figure 8c). Additional analyses of several proteins with altered expression are shown in Ext. Figure 9. All data are mean ± s.d.